January 2015

A Mathematical Investigation Of The Drivers Of Lyme Disease Ecology At Two Ecologically Contrasting Sites

Malia Joy Carpio
Yale University, maliacarpio@gmail.com

A MATHEMATICAL INVESTIGATION OF THE DRIVERS OF LYME DISEASE ECOLOGY AT TWO ECOLOGICALLY CONTRASTING SITES

MALIA CARPIO

MAY 2015

MASTER OF PUBLIC HEALTH | YALE SCHOOL OF PUBLIC HEALTH

ABSTRACT

INTRODUCTION: Lyme disease is an emerging tick-borne disease of increasing concern in the United States. In order to create and to implement effective public health interventions for Lyme disease, there must be a better understanding of the factors driving pathogen transmission.

OBJECTIVES: The primary objectives of this study were to determine how presence/absence of "super-spreaders" and observed differences between two ecologically contrasting sites influence *Borrelia burgdorferi* transmission.

METHODS: A next generation matrix R_0 model was parameterized with field data from an island site (Block Island, Rhode Island) and a mainland site (Connecticut) in order to generate R_0 estimates. A local elasticity analysis was performed in order to identify crucial parameters.

RESULTS: Super-spreaders caused the majority of pathogen transmission but did not greatly influence total transmission. R_0 estimates were greater for the island site than for the mainland site, and island R_0 estimates increased from 2013 to 2014. Model sensitivity to parameter values also varied across sites and years.

CONCLUSION: The dynamics of *B. burgdorferi* transmission may differ across sites and over time within a single site. Additional research is necessary to validate the results of this model and to identify predictors of certain transmission patterns in order to inform public health strategies, particularly as the effects of climate change intensify.

ACKNOWLEDGMENTS

First Reader: Virginia Pitzer, ScD
Second Reader: Maria Diuk-Wasser, PhD

I would like to thank the Yale School of Public Health, the Yale School of Forestry & Environmental Studies, and the Diuk-Wasser Eco-Epidemiology laboratory for the opportunity to conduct tick-borne disease research on Block Island, Rhode Island, during the summers of 2013 and 2014.

Moreover, I am exceedingly grateful to be a recipient of the 2014 Stolwijk Fellowship in Environmental Epidemiology, which funded this study in part.

I wish to extend special thanks to Dr. Maria Diuk-Wasser, Dr. Virginia Pitzer, and Dr. Sarah States, for without their invaluable guidance, contributions, and support, this endeavor would not have been possible.

I am indebted to Dr. Jessica Dunn and Dr. Stephen Davis for the development of the R_0 model and their encouragement and advice for parameterizing it to my data.

I am deeply grateful to Kim Gaffett from the Ocean View Foundation and Scott Comings, Charlotte Herring, and Chris Littlefield from The Nature Conservancy, for without their support, the field work would not have been possible. I would also like to thank Bill Rader and Stephen and Mary Sue Record for graciously allowing me to collect ticks and mice on and adjacent to their properties.

Lastly, I would like to thank my parents, Rey and Beth Carpio, and my sisters, Ané, Liana, and Elissa, for their unwavering support and encouragement in every endeavor I have undertaken.

TABLE OF CONTENTS

LIST OF TABLES

LIST OF FIGURES

INTRODUCTION

Lyme disease is an emerging tick-borne disease and the most commonly reported vector-borne disease in the United States (Bacon et al. 2008). It is of increasing concern in the northeastern and north central regions of the country, and the geographic range may be expanding due to climate change (Ogden et al. 2005; 2006; 2014). Variations in tick phenology, tick population dynamics, and mouse demographics across geographic regions and from year to year may influence the intensity of pathogen transmission. Therefore, it is necessary to understand which factors are most critical for the transmission cycle in order to determine and to mitigate Lyme disease risk for a changing climate and expanded geographic range.

Pathogen transmission is typically characterized by R_0, the basic reproduction number, which represents the number of expected secondary infections produced by one primary case in a totally susceptible, homogenous population. R_0 values that are greater than one indicate that a pathogen can become established in an area, while R_0 values less than one imply that while sporadic outbreaks may occur, they will eventually die out. When estimating spread of a pathogen via R_0, contact rates between infectious and susceptible individuals, duration of infectiousness, and probability of pathogen transmission from an infectious individual to a susceptible individual are generally estimated based on population averages rather than taking individual variation into account (Woolhouse et al. 1997; Lloyd-Smith et al. 2005; Stein 2011). However, ignoring heterogeneities within a population, especially with regard to contact rates, may be problematic for the accurate estimation of disease risk and for the design of effective control policies (Woolhouse et al. 1997; Lloyd-Smith et al. 2005; Stein 2011).

"Super-spreaders," individuals who infect significantly more contacts than the population average, are an increasingly observed phenomenon in infectious disease systems (Woolhouse et al. 1997; Perkins et al. 2003; Ferrari et al. 2004; Meyers et al. 2005; Lloyd-Smith et al. 2005; Small et al. 2006; Kilpatrick et al. 2006; Clay et al. 2009; Stein 2011). Typically following the "20/80 rule," super-spreaders tend to comprise 20% of the population yet cause 80% of total pathogen transmission (Woolhouse et al. 1997; Lloyd-Smith et al. 2005). This type of transmission pattern indicates that the most effective and efficient control strategies will be targeted mainly on the super-spreader subgroup rather than the population as a whole (Woolhouse et al. 1997; Lloyd-Smith et al. 2005; Stein 2011).

Parasites also generally follow the 20/80 rule, with a large proportion of the parasite population aggregating on a small subset of their host population (Perkins et al. 2003; Ferrari et al. 2004; Brunner & Ostfeld 2008; Calabrese et al. 2011; Devevey & Brisson 2012; Johnson & Hoverman 2014). For tick-borne pathogens, this tendency to aggregate may have significant consequences for transmission (Perkins et al. 2003; Brunner & Ostfeld 2008; Calabrese et al. 2011; Harrison & Bennett 2012).

Transmission of tick-borne pathogens can occur by any of three potential routes. The first is vertical or transovarial transmission, in which the infected adult female passes the pathogen on to her eggs, resulting in infected larvae. The second is nonsystemic

transmission, which can occur when two ticks of any life stage are co-feeding in close proximity spatially and temporally on a host. One of the ticks is infectious, and it locally infects the host. The second tick picks up the pathogen, but the infection does not spread throughout the host, and ticks that feed on the same host during a later time period will not be infected. The third is horizontal transmission, in which a host is infected by an infectious tick, develops a systemic infection, and transmits the pathogens to ticks that subsequently feed on it.

Transovarial and nonsystemic transmission have a minor role, if any, in the ecology of *Borrelia burgdorferi*, the causative agent of Lyme disease, in North America (Piesman et al. 1986; Davis & Bent 2011). Horizontal transmission is possible due to the two-year life cycle of *Ixodes scapularis*, the vector of Lyme disease in the eastern United States, which results in a seasonal inversion of nymphal and larval activity (Yuval & Spielman 1990). During the first year, larval ticks take one blood meal during the late summer months, and during the second year, nymphs take one blood meal in the late spring and early summer (Piesman & Spielman 1979; Main et al. 1982; Wilson & Spielman 1985; Yuval & Spielman 1990). Since the seasonal peak of nymphal activity precedes the majority of larval activity, pathogen-infected nymphs can infect small rodent hosts, and the larvae can acquire the pathogen when they feed on the same hosts in the late summer. Thus, the nymphal stage of the tick transmits the infection to the less mature larval stage (Yuval & Spielman 1990).

Since horizontal transmission is dependent upon two tick life stages, co-aggregation of both nymphs and larvae on the same hosts would impact the *B. burgdorferi* cycle. That is, certain hosts would be most likely to become infected from nymphal ticks as well as to transmit the pathogen to larval ticks. Studies investigating pathogen transmission for tick-borne encephalitis virus and *B. burgdorferi* have shown that co-aggregation of ticks on mice is likely to play a significant role in European transmission cycles (Perkins et al. 2003; Harrison & Bennett 2012). However, there has been no investigation of the role of super-spreaders for the North American Lyme disease system. In order to determine how variation across sites and years and the presence/absence of super-spreaders affect pathogen transmission, a next generation matrix (NGM) R_0 model was parameterized from three sets of field data from sites in the northeastern United States.

MATERIALS AND METHODS

R0 Model

Hartemink and colleagues (2008) developed a next generation matrix (NGM) to calculate the basic reproduction number, R_0, for complex tick-borne disease systems. The advantage of this methodology is that it can account for the discrete nature of tick bites and the seasonality of tick activity, and the mathematical calculations retain a clear biological basis (Hartemink et al. 2008). This model has been further simplified for tick-borne pathogens in North America. A loop analysis by Davis and Bent (2011) confirmed that transmission of *B. burgdorferi*, *Babesia microti*, and *Anaplasma phagocytophilium* occurs almost exclusively via the horizontal route in the northeastern United States. Dunn et al. (2013) adapted and parameterized the R_0 model for *B. microti* transmission. Since *B. burgdorferi* and *B. microti*

share the same transmission cycle in the northeastern United States, the R_0 model from Dunn et al. (2013) was parameterized for *B. burgdorferi* ecology for a mainland site (Connecticut) and an island site (Block Island).

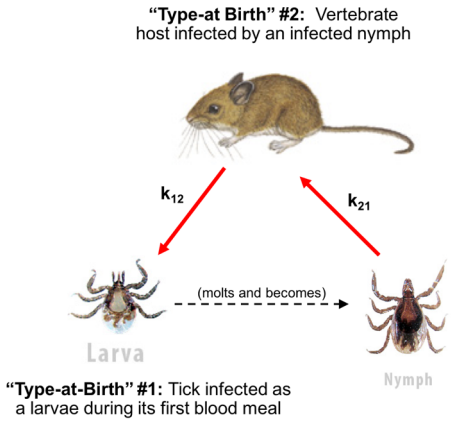

Figure 1. *The simplified transmission cycle of* B. burgdorferi

The "Simple" Case

The NGM approach follows the "birth" of infection in various host species, characterizing them as different "types-at-birth" based on the role of the host in the transmission cycle. The simplified R_0 model defines one tick host type-at-birth and one vertebrate host type-at-birth, resulting in the following NGM ($\boldsymbol{K}$) and R_0 calculation (see also Figure 1):

$$\boldsymbol{K} = \begin{bmatrix} 0 & k_{12} \\ k_{21} & 0 \end{bmatrix} \qquad \text{and} \qquad R_0 = \sqrt{k_{12}k_{21}}$$

where

Host type 1 = tick infected during its first blood meal as a larva

Host type 2 = vertebrate host infected by an infectious nymph

and

k_{12} = Expected # of larvae infected by host type 2

k_{21} = Expected # of vertebrate hosts infected by host type 1

which are given by the equations

$$k_{21} = s_N * q_N * c$$

$$k_{12} = \int_{t=0}^{t=365} a_N(t) \int_{t'=0}^{t'=365-t} \frac{1}{d_L} p(t')\theta \overline{Z}_L(t'+t)dt'dt$$

with parameters defined in Table 1.

The vertebrate host is assumed to be *Peromyscus leucopus*, the white-footed mouse, which is both the most common and competent reservoir host for *B. burgdorferi* (Piesman & Spielman 1979; Main et al. 1982; Donahue et al. 1987; Mather et al. 1989). This generalization is particularly relevant for the ecology of Lyme disease on Block Island due to the simplified host community for the immature stages of *I. scapularis*. Unlike mainland sites, potential hosts are limited to meadow voles, Norway rats, white-footed mice, and various species of birds.

The Co-Aggregated Case

A modified R_0 model can account for "super-spreader" mice by accounting for co-aggregation of larval and nymphal ticks on the same mice. That is, if particular mice provide the majority of nymphal blood meals, then they have a higher probability of becoming infected. If the majority of larval ticks also feed on these same individual mice, then the rate of horizontal transmission would be greater. Therefore, mice with high tick burdens would be "super-spreaders" (Figure 2). The revised R_0 model is given by the following equation:

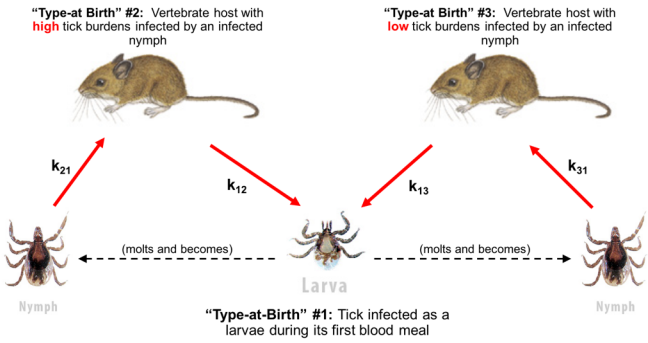

Figure 2. *The co-aggregated transmission cycle of* B. burgdorferi

$$R_0 = \sqrt{k_{12}k_{21} + k_{13}k_{31}}$$

where

Host type 1 = tick infected during its first blood meal as a larva

Host type 2 = vertebrate host with high tick burdens infected by an infectious nymph ("super-spreader")

Host type 3 = vertebrate host with low tick burdens infected by an infectious nymph

and

k_{12} = Expected # of larvae infected by a mouse with high tick burdens

k_{21} = Expected # of mice with high tick burdens infected by a nymph

k_{13} = Expected # of larvae infected by a mouse with low tick burdens

k_{31} = Expected # of mice with low tick burdens infected by a nymph

which are given by the equations

$$k_{21} = m * s_N * q_N * c$$

$$k_{31} = (1 - m) * s_N * q_N * c$$

$$k_{12} = \int_{t=0}^{t=365} a_{NS}(t) \int_{t'=0}^{t'=365-t} \frac{1}{d_L} p(t')\theta \overline{Z}_{LS}(t' + t)dt'dt$$

$$k_{13} = \int_{t=0}^{t=365} a_{NB}(t) \int_{t'=0}^{t'=365-t} \frac{1}{d_L} p(t')\theta \overline{Z}_{LB}(t' + t)dt'dt$$

with parameters defined in Table 1.

Table 1. *A description of parameters for the* R_0 *model*

Parameter	Description
t	time of infection of a mouse
t'	number of days since infection in a single mouse
m	the proportion of ticks feeding on high tick burden mice rather than low tick burden mice (degree of co-aggregation)
s_N	proportion of fed larvae that survive to nymphs
q_N	probability of transmission from infected nymphs to mice
c	proportion of nymphs that successfully find a mammal host (*P. leucopus*)
$a_N(t)$**	proportion of host seeking nymphs that emerge and feed at time t**
$p(t')$	infectivity of hosts as a function of days post infection
θ	mouse survival (the proportion of P. leucopus t' days after infection)
$\overline{Z}_L(t' + t)$**	expected larval burden on mice**
**For co-aggregated model, "S" subscript denotes "high burden mice" and "B" subscript denotes "low burden mice"	

For a full description of the development and simplifying assumptions of the R_0 model, see Appendix B. For a full description of parameter estimation, see Appendices C and D.

Four Model Scenarios

The R_0 model was parameterized for four different scenarios based on the available field data. The following three years of field data were available: 2013 Block Island (Island), 2014 Block Island (Island), and 2014 Connecticut (Mainland). Since the 2013 Island data showed much lower larval spring activity than the 2014 Island data, a second 2014 Island scenario was run without larval spring activity in order to determine the importance of larval spring activity to our estimates of R_0. The model scenarios differed in mouse survivorship, seasonal timing and magnitude of expected tick burdens on mammal hosts, nymphal questing (host-seeking) activity, survivorship of fed larvae from year 1 to year 2, and success of nymphs in finding a mammal host, with all parameter estimates being lower for the Mainland than for the Island (Tables 2, 3, and 4). Simple and co-aggregated R_0 estimates were generated for each model scenario.

Mammal Trapping Field Data

P. leucopus were trapped in Sherman traps at three sites on Block Island, Rhode Island, and four sites in Connecticut. All Connecticut sites had a 12x12 trapping grid, with Sherman traps placed 10 meters apart. Due to site availability, the Block Island sites had a 10x11 trapping grid, 10x6 grid, and 13x4 grid, with Sherman traps placed 10 meters apart. Each trapping session lasted for three consecutives nights/days, and each grid was trapped every other week throughout the duration of the summer. There were seven total trapping sessions for each Block Island grid in 2013 and 2014 and eight total trapping sessions for each Connecticut grid in 2014. For each mouse, the age, sex, weight, reproductive status, blood samples, and nymphal and larval burdens were collected.

Table 2. *Parameter estimates from literature*

Parameter	Point Estimate	Reference
c	0.5	Dunn et al. 2013, Davis and Bent 2011, Piesman and Spielman 1982
s_N	0.4	Dunn et al. 2013, Davis and Bent 2011
q_N	0.83	Dunn et al. 2013, Piesman and Spielman 1982
c^*s_N	0.26	Block Island Field data (Diuk-Wasser, unpublished)

Parameter Estimation

The majority of parameters used in the R_0 model were estimated from field data or laboratory data. Days of larval attachment to a host, d_L, and probability of pathogen transmission from a nymph to a host, q_N, were taken from the literature for all four model scenarios (Table 2). For the Mainland 2014 scenario, parameter values for c and s_N were also taken from the literature (Table 2). For all Island scenarios, the product of c and s_N was estimated from two consecutive years of field data (Table 2, Appendix D).

Expected Tick Burdens

The expected (mean) number of ticks on a mammal host on day t of the year was determined using the methods developed by Brunner and Ostfeld (2008) and employed by Dunn et al. (2013). Tick count data was assumed to follow a zero-inflated, over-dispersed negative binomial distribution on each trapping day with dispersion parameter α and mean $\mu(t_i)$. While the dispersion parameter was assumed to be constant throughout the entire year, the mean was assumed to vary and to be described by $\bar{Z}_N(t)$ for nymphal burden and $\bar{Z}_L(t)$ for larval burden. The types of curves and all parameters for all four scenarios (for both simple and co-aggregated R_0 models) are shown in Tables 3 and 4, and examples of $\bar{Z}_N(t)$ and $\bar{Z}_L(t)$ and how the curves are affected by the parameter values are shown in Figure 3 (See also Appendix C). Co-aggregated burdens for "super-spreader" mice were determined using the burden data from the top 20% of mice with the highest nymphal burdens or the top 20% of mice with the highest larval burdens (since the highest nymphal and highest larval burdens did not necessarily occur on the same mice). Co-aggregated burdens for "non-super-spreaders" were determined using the burden data from the bottom 80% of mice with the lowest nymphal or larval burdens.

Infectivity of Mice as a Function of Days Post Infection

A mouse infected with *B. burgdorferi* will be infectious to nymphs at different levels throughout the duration of infection. The data used to estimate the infectivity of *P. leucopus* as a function of days post infection was from a transmission experiment conducted at the Diuk-Wasser laboratory (States, unpublished data). For eight different time points spanning a period of 100 days, 100 uninfected larvae were allowed to feed on *P. leucopus* hosts infected with *B. burgdorferi* strain ospC type C. Larvae were collected and allowed to molt into nymphs, which were then tested for infection. From a total of 215 molted and tested nymphs, the proportion of infected ticks at each feeding time point was recorded. The mean infection prevalence curves were estimated via a log-normal distribution and fit using the same methodology as the tick burden curves (Table 5, Figure 4, see also Appendix D).

Table 3. *Type of curve and parameter estimates for the expected nymphal burdens*

Data Set	Type of Curve	Height	τ^1	μ^2	σ^3	α^4
Mainland Overall	Log Normal	1.3	103.6	58.2	0.4	0.5
Mainland High Burden	Log Normal	2.2	132.3	18.6	0.9	0.2
Mainland Low Burden	Log Normal	0.4	133.3	8.7	2.4	0.0
Island 2014 Overall	Normal	7.8	142.6	19.7	24.5	0.8
Island 2014 High Burden	Log Normal	14.7	135.5	19.0	0.7	0.5
Island 2014 Low Burden	Normal	4.6	138.3	23.8	25.8	0.4
Island 2013 Overall	Normal	4.6	140.1	24.8	21.8	0.7
Island 2013 High Burden	Normal	6.7	133.6	33.5	20.6	0.8
Island 2013 Low Burden	Normal	2.9	134.2	27.2	25.2	0.2

[1]τ = days until start of nymphal activity; [2]μ = days from start to peak of nymphal activity;
[3]σ = shape parameter affecting duration; [4]α = dispersion parameter for negative binomial distribution

Table 4. *Type of curve and parameter estimates for the expected larval burdens*

Data Set	Curve	Spring Height	Spring τ^1	Spring μ^2	Spring σ^3	Fall Height	Fall τ	Fall μ	Fall σ	α^4
Mainland Overall	Log Normal Normal	2.5	129.9	18.6	0.8	13.3	200.8	27.8	15.4	0.7
Mainland High Burden	Log Normal Normal	2.1	135.1	15.4	0.8	18.3	199.0	29.1	16.3	0.5
Mainland Low Burden	Log Normal Normal	2.5	131.1	16.9	0.9	7.6	190.0	37.9	13.7	0.5
Island 2014 Overall	Uniform Log Normal	2.1	141.7	---	---	61.9	203.3	11.9	0.8	0.9
Island 2014 High Burden	Log Normal Log Normal	3.9	144.0	0.3	3.4	122.7	183.0	34.2	0.3	0.4
Island 2014 Low Burden	Linear Normal	---	143.0	---	---	24.6	207.0	13.7	21.3	0.6
Island 2013 Overall	Uniform Normal	0.3	142.6	---	---	48.5	182.5	27.9	11.7	0.6
Island 2013 High Burden	Uniform Normal	0.4	143.0	---	---	58.1	193.0	26.2	12.0	0.6
Island 2013 Low Burden	Uniform Normal	0.3	140.2	---	---	30.8	192.6	30.4	14.6	0.5

[1]τ = days until start of larval activity; [2]μ = days from start to peak of larval activity;
[3]σ = shape parameter affecting duration; [4]α = dispersion parameter for negative binomial distribution

Table 5. *The parameter estimates for the log-normal infection curve for* B. burgdorferi *ospC type C*

***B. burgdorferi* Osp C**	**Height**	**μ**	**σ**	**α**
Type C	1	23.3	1.1	0.0016

Table 6. *Demographics and Survivorship of* P. leucopus *estimated from field data*

Site	% Female	Female Survivorship	Male Survivorship	Overall Survivorship
Mainland 2014	39%	0.642	0.634	0.637
Island 2014	36%	0.894	0.827	0.851
Island 2013	51%	0.771	0.760	0.765

Survival of White-Footed Mice Post Infection

The survival of white-footed mice was estimated from the field data via Program MARK. If the survival estimates differed for males and females, then the average overall survival was weighted by sex (Table 6, Appendix D). The survivorship estimates are only valid for the duration of the field season (May through August). However, these survivorship estimates should be sufficient for the purposes of the R_0 model because infection calculations are limited by the duration of tick activity and the infectivity of mice to nymphs (Appendix C; Appendix D).

Sensitivity/Elasticity Analysis

A one-way sensitivity analysis was performed by varying one parameter value while keeping all other parameters constant. However, since sensitivity values are influenced by the unit values of the parameter in question, the elasticity values are reported instead for comparison across parameters and scenarios. Elasticity is a measure of the relative change in R_0 for a proportional change in one parameter value. With the exception of the parameter denoting the degree of co-aggregation (m), the elasticity analysis was performed for the simple R_0 models. Full results with sensitivity values can be found in Appendix E.

Empirical Evidence for Co-Aggregation

In order to determine empirically if co-aggregation is occurring in the *B. burgdorferi* transmission cycle, we would expect a subset of mice to have significantly higher nymphal

Figure 3. *Examples of the expected nymphal (a) and larval (b) burden curves*

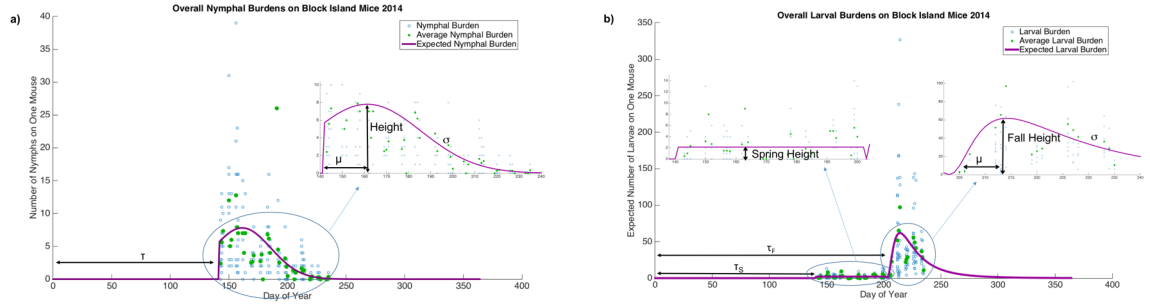

Figure 4. *The infectivity of mice to ticks as a function of days post infection*

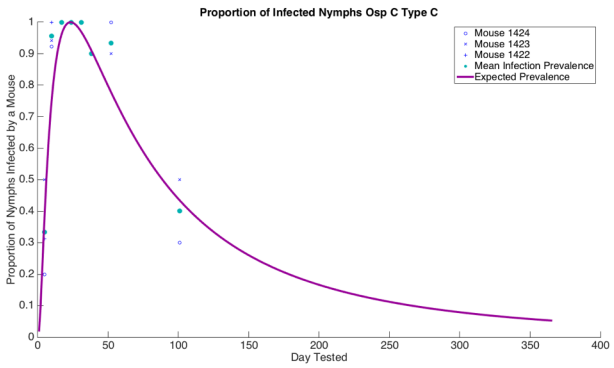

and larval burdens than the rest of the mice. Furthermore, the nymphal and larval burdens should be positively correlated, so that the mice with the highest nymphal burdens also have the highest larval burdens and the mice with the lowest nymphal burdens also have the lowest larval burdens. However, these burdens need not occur during the same time period since horizontal transmission is dependent on systemic infection that persists throughout the summer.

The challenge in determining this relationship from field data is that nymphs and larvae most actively seek hosts at different times during the year, and not all mice were trapped during both of these time periods. Therefore, the data sets were restricted to a subset of individual mice that were captured and re-captured during periods of both nymphal and larval host-seeking activity. After this restriction, there was insufficient data for analysis for 2013 Block Island. For the 2014 Block Island data, there were thirty-three individual mice caught throughout the duration of the summer; for the 2014 Connecticut data, there were 159 individual mice caught throughout the duration of the summer. These data were further divided into "co-aggregation" subgroups of 40/60, 30/70, 20/80, 10/90, and 5/95 (Mainland only), with x% as high burden mice/y% as low burden mice.

The high tick burden mice were determined by sorting according to *larval* burdens and examining the relationship between the nymphal and larval burdens from the top 10%, 20%, 30% or 40% mice compared to the bottom y% (top two rows in Tables 7 and 8). Since the highest larval burdens did not always co-occur with the highest nymphal burdens, a second round of tests was also performed by comparing the nymphal burdens on mice sorted according to high vs. low *nymphal* burdens (last row in Tables 7 and 8).

Since these data were not normally distributed and the subgroup sample sizes were small, Wilcoxon Rank Sum tests were performed to determine if the median tick burden of "high burden" mice was significantly higher than the median tick burden of "low burden" mice (Tables 7 and 8). A two-way test was used in order to generate conservative p-values, and medians were compared in order to confirm that the "high burden" mice did indeed have a greater number of ticks than "low burden" mice (See Appendix D for median values). A Spearman's Rank Order Correlation was also calculated for the subgroups of mice in order to determine if nymphal and larval burdens were positively correlated.

Table 7. *The p-values of the Wilcoxon Rank Sum Test for Block Island*

Island 2014	**90-10%**	**80-20%**	**70-30%**	**60-40%**
Larvae	0.006	<0.001	<0.001	<0.001
Nymphs	0.443	0.455	0.358	0.027
By Nymphs	0.005	<0.001	<0.001	<0.001

Table 8. *The p-values of the Wilcoxon Rank Sum Test for Connecticut*

Mainland 2014	**95-5%**	**90-10%**	**80-20%**	**70-30%**	**60-40%**
Larvae	<0.001	<0.001	<0.001	<0.001	<0.001
Nymphs	0.336	0.917	0.146	0.003	<0.001
By Nymphs	<0.001	<0.001	<0.001	<0.001	<0.001

RESULTS

R_0 Estimates

R_0 estimates were greater for all three Island scenarios than for the Mainland scenario (Table 9). Spring larval activity seemed to have very little effect on R_0, as the estimates for both Island 2014 scenarios were similar despite the presence/absence of spring larvae (Table 9). In the presence of 20/80 co-aggregation, R_0 estimates increased slightly for the Mainland 2014 and Island 2013 scenarios but decreased slightly for both Island 2014 scenarios (Table 9).

Comparing the expected number of secondary infections from "super-spreader" vs. non "super-spreader" hosts showed that mice with high tick burdens contribute much more to pathogen transmission than mice with low tick burdens (Tables 10 and 11). The ratio k_{21}/k_{31} indicates that super-spreader mice are 4 times as likely to become infected as non super-spreaders, as estimated for all four scenarios (Table 10). The ratio k_{12}/k_{13} indicates that super-spreaders are expected to infect 9-17 times as many larvae as non super-spreaders, depending on the scenario (Table 10). R_0 estimates from the 20/80 co-aggregation model with and without the subgroup of high tick burden mice show that super-spreaders are responsible for the majority of pathogen transmission (Table 11).

Elasticity Analysis

The elasticity analysis showed that all model scenarios were responsive to changes in mouse survival post infection, θ; survivorship of larvae from year 1 to year 2, s_n; and probability of nymphs for finding a suitable host, c (Table 12). The Island 2013 model was

Table 9. *The overall and co-aggregated* R_0 *estimates for all four model scenarios*

R_0 Calculation	**Mainland 2014**	**Island 2014**	**Island 2013**	**Island 2014 (No Spring)**
Simple	1.33	11.35	4.50	11.15
20/80 Co-Aggregation	1.38	10.95	4.85	10.88

Table 10. *The ratio of expected secondary infections from super-spreaders and non super-spreaders in mice and ticks for all four model scenarios*

80-20% CoAg	**Mainland 2014**	**Island 2014**	**Island 2013**	**Island 2014 (No Spring)**
k_{21}/ k_{31}	4	4	4	4
k_{12}/ k_{13}	9	9	16	17

Table 11. *Co-Aggregated* R_0 *estimates in the presence/absence of the super-spreader subpopulation*

R_0 Calculation	**Mainland 2014**	**Island 2014**	**Island 2013**	**Island 2014 (No Spring)**
20/80 Rule	1.38	10.95	4.85	10.88
No Super-spreaders	0.23	1.83	1.84	1.33
Only Super-spreaders	1.36	10.80	4.48	10.80

less responsive to the degree of co-aggregation, m, than all other model scenarios, with a roughly linear relationship between m and R_0 (Table 12, Figures 5-8).

The elasticity of the models for expected tick burdens varied greatly across the four scenarios (Table 12). The Mainland 2014 model was responsive to the duration of spring and fall larval activity peaks, while the Island 2014 model was not responsive to any of the expected tick burdens. In the absence of a spring larval peak, the Island 2014 model became more responsive to the height of the fall larval burden peak. The Island 2013 model was most responsive to expected tick burdens, especially the duration of the nymphal activity and fall larval activity (Table 12). The differences in elasticities across the four scenarios is likely due to the variation in the type of curves that best estimated the expected larval and nymphal burdens based on the field data, as well as the timing of larval and nymphal peak activity (Tables 3 and 4).

Evidence for Co-Aggregation from the Field Data

When sorted separately according to larval burden or nymphal burden, median larval or nymphal burdens are significantly greater for "high burden" mice than for "low burden" mice for all ratios of co-aggregation at both Island and Mainland sites (first and last rows in Tables 7 and 8). However, if mice are sorted into "high" or "low" burden categories by larval burden, and their nymphal burdens are compared, the results vary. For the Island, nymphal burdens are only significantly greater for high burden mice when these mice account for 40% of the population (middle row in Table 7). For the Mainland, nymphal burdens are significantly greater for high burden mice when these mice account for 30% of the population or greater (middle row in Table 8). The Spearman Rank Order Correlation showed a positive correlation between nymphal and larval burdens for both the Island and Mainland data, but only the Mainland data was statistically significant ($p_{Mainland} = 0.02$; $p_{Island} = 0.21$). This suggests that aggregation of larvae and nymphal ticks on a subset of mice is occurring, but the co-aggregation of both larval and nymphal ticks on the same subset of mice may depend on the defined ratio of high/low burden mice in the population. There is statistically significant evidence for co-aggregation at a 30/70 ratio on the Mainland and suggestive evidence at a 20/80 ratio. The Island data is not suggestive of co-aggregation, but this may be due to the small sample size (33 mice).

Table 12. *The results of the elasticity analysis for all four model scenarios; notable elasticity values are bolded.*

Parameter	Mainland 2014	Island 2014	Island 2013	Island 2014 (no Spring)
C^*S_n	**0.41**	**0.37**	**0.40**	**0.41**
$\theta^{t'}$	**0.47**	**0.46**	**0.47**	**0.47**
Nymphal Height	0.00	0.00	0	0.00
Nymphal Sigma	-0.04	-0.03	**1.84**	-0.03
Spring Larval Height	0.01	0.15	0	---
Spring Larval Sigma	**0.44**	0.02	---	---
Fall Larval Height	0.10	0.16	**0.41**	**0.46**
Fall Larval Sigma	**0.41**	0.00	**0.88**	0.10
m	**0.40**	**0.40**	0.12	**0.43**

Figures 5 – 8. *The Co-Aggregated* R_0 *estimates as a function of proportion of ticks feeding on high burden (super-spreader) mice for all model scenarios*

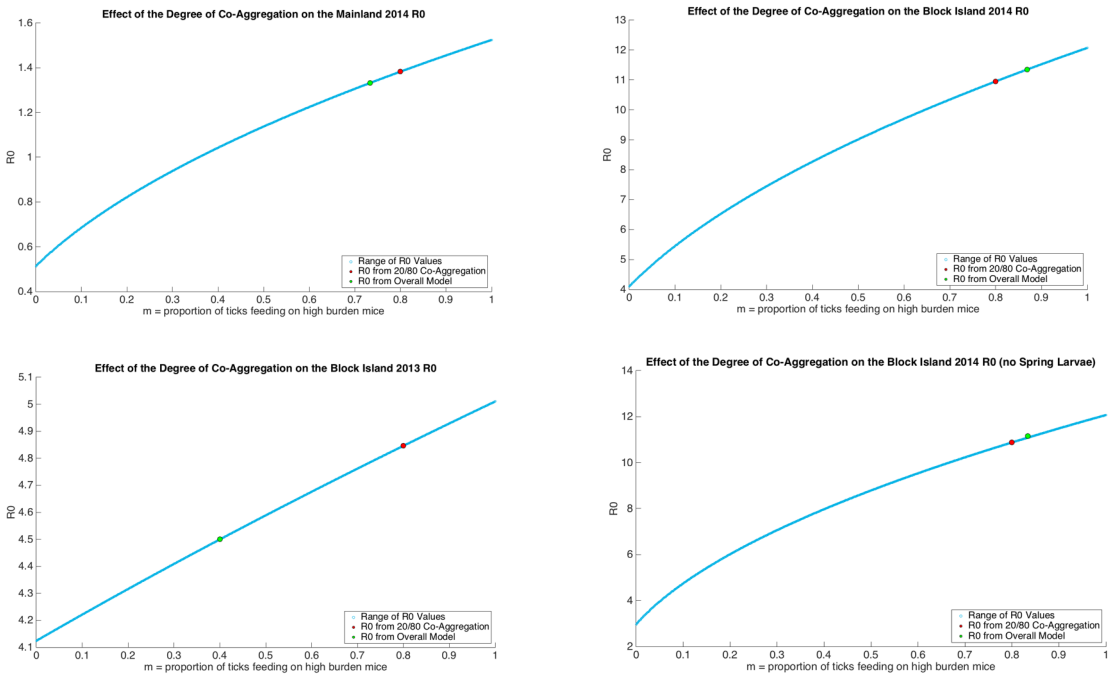

DISCUSSION

Many studies have shown that the transmission cycle of *B. burgdorferi* is dependent on several biotic and abiotic factors, which may vary across sites and years (reviewed in Kurtenbach et al. 2006). The R_0 model results presented here are consistent with this knowledge, as the intensity of pathogen transmission and the most influential parameters differed for the four scenarios. Temperature and relative humidity are known to influence the extrinsic incubation period (i.e. duration of development from larva to nymph), daily and seasonal tick survivorship, host-seeking activity of ticks, and the degree of synchronicity of larval and nymphal seasonal activity (Yuval & Spielman 1990; Stafford 1994; Lindsay et al. 1995; Bertrand & Wilson 1996; Ginsberg & Zhioua 1996; Wilson 1998; Vail & Smith 2002; Ogden et al. 2004; Kurtenbach et al. 2006). Climatic variations in concert with composition and abundance of host community, degree of landscape heterogeneity, and host behavioral differences are likely to determine the expected tick burden on hosts for a given site in a given year and therefore *B. burgdorferi* transmission.

Role of Super-Spreaders

Unlike the R_0 model results from Harrison and Bennett (2012), presence of super-spreaders did not uniformly increase total pathogen transmission, as indicated by the R_0 estimates (Table 9). However, as expected, co-aggregation of ticks did increase the probability that a high burden mouse would become infected and transmit the pathogen to larvae (Table 10). These super-spreader mice were responsible for the majority of pathogen transmission for

all four scenarios, indicating that the most efficacious and cost-effective disease control strategies should be targeted at this subpopulation (Table 11, Woolhouse et al. 1997; Lloyd-Smith et al. 2005).

Field data from both mainland and island sites shows that certain mice have significantly higher nymphal and larval burdens than the rest of the population (Tables 7 and 8). Evidence for co-aggregation of both nymphs and larvae on the same mice is not as supportive (Tables 7 and 8). The data from the mainland site is more suggestive of co-aggregation than the island site, at least for a 30/70 ratio (Tables 7 and 8, Spearman Rank Order Correlation $p_{Mainland} = 0.02$, $p_{Island} = 0.21$). However, the non-statistically significant results for Block Island 2014 could be due to the small sample size (33 mice). Additional studies are necessary to determine whether or not there are super-spreaders in the North American Lyme disease cycle at ecologically contrasting sites.

Spring Larval Activity on Block Island

The difference in the empirical data on spring larval activity for Block Island from 2013 to 2014 may have been due to differences in winter weather and unfed larval survivorship. During the winter of 2013-2014, Block Island received snow cover, a somewhat rare event, which may have contributed to increased larval survivorship and the presence of a spring larval peak (Lindsay et al. 1995). While the removal of a spring larval peak did not significantly alter R_0 estimates for the Island 2014 scenarios, the 2013 and 2014 model scenarios were sensitive to different parameters (Table 12). Therefore, spring larval peak may play a significant role in pathogen transmission only under certain conditions but not under all possible conditions. If this is the case, then altered weather patterns, such as increased/decreased snowfall may or may not influence tick-borne disease dynamics.

Model Limitations

While the R_0 models we explore here account for several important aspects of *B. burgdorferi* transmission, such as the discrete nature of tick bloodmeals and the seasonality of nymphal and larval activity, there are additional factors that can influence transmission that have not been taken into account. For example, the models do not account for the possibility that mice may be re-infected throughout the year, increasing their infectivity to larvae. We also do not account for co-infection of mice and ticks by multiple strains of *B. burgdorferi* or multiple pathogens, which may affect duration of infectiousness and probability of pathogen transmission from mice to ticks. Furthermore, super-spreaders are defined in terms of increased rates of contact between mice and ticks but not in terms of "super-shedders," or mice which are more infectious than others due to immunological differences. Lastly, our models do not account for a possible "dilution" effect from ticks feeding on mammal hosts that are less competent reservoirs for *B. burgdorferi* than *P. leucopus*. Block Island has a simplified host community that lacks many of the potential "dilution" hosts that are present in the Connecticut sites, so this is less of a limitation for the Island scenarios.

Some of these factors might be accounted for with additional data, such as data on "super-shedding," but the addition of the possibility of re-infection and co-infections would require a more complex version of the model. Investigation of whether or not there is a "dilution"

effect could be accomplished through an improved estimate for the parameter, *c*, which denotes the probability of nymphs successfully finding a *P. leucopus* host, or through including additional, less competent "types-at-birth" in the NGM.

CONCLUSION

This study shows that the ecology of *B. burgdorferi* transmission can vary greatly for two geographic sites and across years for the same geographic site. While there do seem to be a few unifying factors influencing transmission for all geographic locations across the years, the effect of tick burdens on hosts varies greatly (Table 12). Therefore, to mitigate *B. burgdorferi* transmission effectively, one may have to alter the type and the amount of effort of a public health intervention according to specific spatiotemporal circumstances. For example, although larval survivorship seems to be a universally critical parameter, if larval survivorship is targeted as a control strategy via application of acaricides, the models suggest that the level of effort required to stop Lyme disease outbreaks in Connecticut will be less than the effort required to stop outbreaks on Block Island.

Presence of super-spreaders should radically alter any disease mitigation strategies, with all interventions targeted at the super-spreader subpopulation in order to maximize effectiveness (Tables 10 and 11). Further investigation is necessary to confirm the role of super-spreaders in *B. burgdorferi* transmission under multiple conditions (e.g. differing mouse densities, heterogeneous vs. homogeneous landscapes). Conflicting results on the effect of intrinsic host characteristics (e.g. age, sex, body size) and the spatial aggregation of immature ticks in the environment causing aggregation of ticks on hosts suggests that super-spreaders may be the product of several factors, including temporal, spatial, and individual-specific variables (Brunner & Ostfeld 2008; Calabrese et al. 2011; Devevey & Brisson 2012). However, if this suite of interacting influences can be characterized to a sufficient degree, it could inform and dramatically increase the efficacy of Lyme disease control strategies.

For example, mouse vaccination has been found to be effective in reducing infection prevalence in nymphs, but it has not been able to disrupt the transmission cycle to an acceptably low level (Tsao et al. 2004; Tsao et al. 2012). These mediocre results may be due to a failure to target the super-spreader population rather than a failure of the intervention itself. Furthermore, if spatial aggregation of ticks in the environment is determined to be one of the causative factors for super-spreader mice, targeted application of acaricides in tandem with vaccination may effectively intervene in the *B. burgdorferi* transmission cycle (Calabrese et al. 2011).

Current *B. burgdorferi* transmission cycles may be significantly altered by the impending effects of climate change, such as increased snowfall that may result in higher larval survivorship and increases in larval spring activity. Continued research is necessary to monitor if and how the disease ecology changes with alterations to temperature and precipitation patterns for a specific geographic site across multiple years.

WORKS CITED

Bacon, R. M., K. J. Kugeler, P. S. Mead, Centers for Disease Control and Prevention (CDC). 2008. Surveillance for Lyme disease--United States, 1992-2006. Morbidity and mortality weekly report. Surveillance summaries (Washington, D.C. : 2002) **57**:1–9.

Bertrand, M. R., and M. L. Wilson. 1996. Microclimate-dependent survival of unfed adult Ixodes scapularis (Acari: Ixodidae) in nature: life cycle and study design implications. Journal of medical entomology.

Brunner, J. L., and R. S. Ostfeld. 2008. Multiple causes of variable tick burdens on small-mammal hosts. Ecology **89**:2259–2272.

Calabrese, J. M., J. L. Brunner, and R. S. Ostfeld. 2011. Partitioning the aggregation of parasites on hosts into intrinsic and extrinsic components via an extended Poisson-gamma mixture model. PLoS ONE **6**:e29215.

Clay, C. A., E. M. Lehmer, A. Previtali, S. St Jeor, and M. D. Dearing. 2009. Contact heterogeneity in deer mice: implications for Sin Nombre virus transmission. Proceedings. Biological sciences / The Royal Society **276**:1305–1312.

Davis, S., and S. J. Bent. 2011. Loop analysis for pathogens: niche partitioning in the transmission graph for pathogens of the North American tick Ixodes scapularis. Journal of Theoretical Biology **269**:96–103.

Devevey, G., and D. Brisson. 2012. The effect of spatial heterogenity on the aggregation of ticks on white-footed mice. Parasitology **139**:915–925.

Donahue, J. G., J. Piesman, and A. Spielman. 1987. Reservoir competence of white-footed mice for Lyme disease spirochetes. The American journal of tropical medicine and hygiene **36**:92–96.

Dunn, J. M., S. Davis, A. Stacey, and M. A. Diuk-Wasser. 2013. A simple model for the establishment of tick-borne pathogens of Ixodes scapularis: a global sensitivity analysis of R0. Journal of Theoretical Biology **335**:213–221.

Ferrari, N., I. M. Cattadori, J. Nespereira, A. Rizzoli, and P. J. Hudson. 2004. The role of host sex in parasite dynamics: field experiments on the yellow-necked mouse Apodemus flavicollis. Ecology letters **7**:88–94.

Ginsberg, H. S., and E. Zhioua. 1996. Nymphal survival and habitat distribution of Ixodes scapularis and Amblyomma americanum ticks (Acari: Ixodidae) on Fire Island, New York, USA. Experimental & Applied Acarology **20**:533–544. Kluwer Academic Publishers.

Harrison, A., and N. C. Bennett. 2012. The importance of the aggregation of ticks on small mammal hosts for the establishment and persistence of tick-borne pathogens: an investigation using the R(0) model. Parasitology **139**:1605–1613.

Hartemink, N. A., S. E. Randolph, S. A. Davis, and J. A. P. Heesterbeek. 2008. The basic reproduction number for complex disease systems: defining R(0) for tick-borne infections. The American naturalist **171**:743–754.

Johnson, P. T. J., and J. T. Hoverman. 2014. Heterogeneous hosts: how variation in host size, behaviour and immunity affects parasite aggregation. The Journal of animal ecology.

Kilpatrick, A. M., P. Daszak, M. J. Jones, P. P. Marra, and L. D. Kramer. 2006. Host heterogeneity dominates West Nile virus transmission. Proceedings. Biological sciences The Royal Society **273**:2327–2333.

Kurtenbach, K., K. Hanincová, J. I. Tsao, G. Margos, D. Fish, and N. H. Ogden. 2006. Fundamental processes in the evolutionary ecology of Lyme borreliosis. Nature reviews. Microbiology **4**:660–669.

Lindsay, L. R., I. K. Barker, G. A. Surgeoner, S. A. McEwen, T. J. Gillespie, and J. T. Robinson. 1995. Survival and development of Ixodes scapularis (Acari: Ixodidae) under various climatic conditions in Ontario, Canada. Journal of medical entomology **32**:143–152.

Lloyd-Smith, J. O., S. J. Schreiber, P. E. Kopp, and W. M. Getz. 2005. Superspreading and the effect of individual variation on disease emergence. Nature **438**:355–359.

Main, A. J., A. B. Carey, M. G. Carey, and R. H. Goodwin. 1982. Immature Ixodes dammini (acari: Ixodidae) on small animals in Connecticut, USA. Journal of medical entomology **19**:655–664.

Mather, T. N., M. L. Wilson, S. I. Moore, J. M. Ribeiro, and A. Spielman. 1989. Comparing the relative potential of rodents as reservoirs of the Lyme disease spirochete (Borrelia burgdorferi). American Journal of Epidemiology **130**:143–150.

Meyers, L. A., B. Pourbohloul, M. E. J. Newman, D. M. Skowronski, and R. C. Brunham. 2005. Network theory and SARS: predicting outbreak diversity. Journal of Theoretical Biology **232**:71–81.

Ogden, N. H., A. Maarouf, I. K. Barker, M. Bigras-Poulin, L. R. Lindsay, M. G. Morshed, C. J. O'Callaghan, F. Ramay, D. Waltner-Toews, and D. F. CHARRON. 2006. Climate change and the potential for range expansion of the Lyme disease vector Ixodes scapularis in Canada. International Journal for Parasitology **36**:63–70.

Ogden, N. H., L. R. Lindsay, G. Beauchamp, D. Charron, A. Maarouf, C. J. O'Callaghan, D. Waltner-Toews, and I. K. Barker. 2004. Investigation of relationships between temperature and developmental rates of tick Ixodes scapularis (Acari : Ixodidae) in the laboratory and field. Journal of medical entomology **41**:622–633.

Ogden, N. H., M. Bigras-Poulin, C. J. O'Callaghan, I. K. Barker, L. R. Lindsay, A. Maarouf, K. E. Smoyer-Tomic, D. Waltner-Toews, and D. Charron. 2005. A dynamic population model to investigate effects of climate on geographic range and seasonality of the tick Ixodes scapularis. International Journal for Parasitology **35**:375–389.

Ogden, N. H., M. Radojević, X. Wu, V. R. Duvvuri, P. A. Leighton, and J. Wu. 2014. Estimated effects of projected climate change on the basic reproductive number of the Lyme disease vector Ixodes scapularis. Environmental Health Perspectives **122**:631–638.

Perkins, S. E., I. M. Cattadori, V. Tagliapietra, A. P. Rizzoli, and P. J. Hudson. 2003. Empirical evidence for key hosts in persistence of a tick-borne disease. International Journal for Parasitology **33**:909–917.

Piesman, J., and A. Spielman. 1979. Host-associations and seasonal abundance of immature Ixodes dammini in southeastern Massachusetts. Annals of the Entomological ….

Piesman, J., J. G. Donahue, T. N. Mather, and A. Spielman. 1986. Transovarially acquired Lyme disease spirochetes (Borrelia burgdorferi) in field-collected larval Ixodes dammini (Acari: Ixodidae). Journal of medical entomology **23**:219.

Small, M., C. K. Tse, and D. M. Walker. 2006. Super-spreaders and the rate of transmission of the SARS virus. Physica D: Nonlinear Phenomena **215**:146–158.

Stafford, K. C., III. 1994. Survival of immature Ixodes scapularis (Acari: Ixodidae) at different relative humidities. Journal of medical entomology **31**:310–314.

Stein, R. A. 2011. Super-spreaders in infectious diseases. International journal of infectious diseases : IJID : official publication of the International Society for Infectious Diseases **15**:e510–3.

Tsao, J. I., J. T. Wootton, J. Bunikis, M. G. Luna, D. Fish, and A. G. Barbour. 2004. An ecological approach to preventing human infection: Vaccinating wild mouse reservoirs intervenes in the Lyme disease cycle. Proceedings of the National Academy of Sciences of the United States of America **101**:18159–18164.

Tsao, K., D. Fish, and A. P. Galvani. 2012. Predicted outcomes of vaccinating wildlife to reduce human risk of Lyme disease. Vector borne and zoonotic diseases (Larchmont, N.Y.) **12**:544–551.

Vail, S. G., and G. Smith. 2002. Vertical Movement and Posture of Blacklegged Tick (Acari: Ixodidae) Nymphs as a Function of Temperature and Relative Humidity in Laboratory Experiments. Journal of medical entomology **39**:842–846.

Wilson, M. L. 1998. Distribution and abundance of Ixodes scapularis (Acari: Ixodidae) in North America: ecological processes and spatial analysis. Journal of medical entomology **35**:446–457.

Wilson, M. L., and A. Spielman. 1985. Seasonal activity of immature Ixodes dammini (Acari: Ixodidae). Journal of medical entomology **22**:408–414.

Woolhouse, M. E. et al. 1997. Heterogeneities in the transmission of infectious agents: implications for the design of control programs. Proceedings of the National Academy of Sciences of the United States of America **94**:338–342.

Yuval, B., and A. Spielman. 1990. Duration and regulation of the developmental cycle of Ixodes dammini (Acari: Ixodidae). Journal of medical entomology **27**:196–201.

APPENDICES A – F

LIST OF APPENDICES

APPENDIX A.

Overview of Lyme Disease Ecology

In the northeastern and north central United States, the blacklegged tick, *Ixodes scapularis*, is the vector for *Borrelia burgdorferi*, the causative agent of Lyme disease. It has a two-year life cycle with the four life stages of egg, larva, nymph, and adult (Spielman et al. 1985). The tick takes one blood meal during each life stage as larva, nymph, and adult (only females feed during the adult stage) (Spielman et al. 1985). The adults feed almost exclusively on *O. virginianus*, and the presence of *I. scapularis* populations depends on the presence of *O. virginianus* populations (Piesman & Spielman 1979; Main et al. 1981; Wilson et al. 1984; Spielman et al. 1985; Wilson & Spielman 1985; Wilson 1998). While *O. virginianus* are essential as reproductive hosts for *I. scapularis*, they are not competent reservoirs for *B. burgdorferi* (Telford et al. 1988; Steere et al. 2004). Immature ticks feed mainly on small mammals and birds (Spielman et al. 1985). The white-footed mouse, *Peromyscus leucopus*, is the most competent and the most common reservoir host, though a wide range of mammals and bird species have been identified as reservoir hosts with varying levels of competence (Piesman & Spielman 1979; Main et al. 1982; Donahue et al. 1987; Mather et al. 1989).

Transmission of tick-borne pathogens can occur by any of three potential routes. The first is vertical or transovarial transmission, in which the infected adult female passes the pathogen on to her eggs, resulting in infected larvae. The second is nonsystemic transmission, which can occur when two ticks of any life stage are co-feeding in close proximity spatially and temporally on a host. One of the ticks is infectious, and it locally infects the host. The second tick picks up the pathogen, but the infection does not spread throughout the host, and ticks that feed on the same host during a later time period will not be infected. The third is horizontal transmission, in which a host is infected by an infectious tick, develops a systemic infection, and transmits the pathogens to ticks that subsequently feed on it.

Horizontal transmission is possible due to the two-year life cycle of *I. scapularis*, which results in a seasonal inversion of nymphal and larval activity (Yuval & Spielman 1990). During the first year, larval ticks take one blood meal during the late summer months, and during the second year, nymphs take one blood meal in the late spring and early summer (Yuval & Spielman 1990, Kurtenbach et al. 2006). Since the seasonal peak of nymphal activity precedes the majority of larval activity, pathogen-infected nymphs can infect small rodent hosts, and the larvae will acquire the pathogen when they feed in the late summer. Thus, the nymphal stage of the tick transmits the infection to the less mature stage (Yuval & Spielman 1990).

As might be expected, modeling the ecology of *B. burgdorferi* can quickly become complex and require a large number of parameters – two factors that make it difficult to keep the model grounded in the basis of field-collected data (Dunn 2014). It is also important to account for the seasonality of tick activity according to life stage, the aggregation of ticks on hosts, and the fact that ticks feed once per life stage and do not have a continuous biting rate (Dunn 2014).

APPENDIX B.

Background on the Development of the R_0 Model

THE R_0 MODEL – A NEXT GENERATION MATRIX

Hartemink and colleagues (2008) developed a next generation matrix (NGM) to calculate the basic reproductive number for complex tick-borne disease systems. The advantage of this methodology is that it can account for the discrete nature of tick bites, and the mathematical calculations retain a clear biological basis (Hartemink et al. 2008). First, the following five different infectious "types-at-birth" were identified:

1) Tick infected as an egg from transovarial transmission
2) Tick infected as a larva during the first blood meal
3) Tick infected as a nymph during the second blood meal
4) Tick infected as an adult during the third blood meal
5) A systemically infectious vertebrate host (allows for horizontal transmission)

These types-at-birth refer to the birth of the *infection* in the ticks and vertebrate hosts rather than the birth of actual individuals (Hartemink et al. 2008) . Therefore, non-competent vertebrate hosts such as *O. virginianus* cannot be included in the NGM because they do not become infected and cannot give rise to other new infections. However, they may still play an important role in disease transmission if they serve as a source of "dilution" and/or as a source of blood meals to sustain the tick population.

The types-at-birth are entered into the matrix **K** with elements k_{ij}, where each element represents the expected number of secondary cases in type-at-birth i caused by an infectious individual with type-at-birth j. However, not all types-at-birth can infect other types-at-birth, and in those cases, $k_{ij} = 0$. Therefore, the next generation matrix **K** is as follows (Hartemink et al. 2008):

$$\boldsymbol{K} = \begin{bmatrix} k_{11} & k_{12} & k_{13} & k_{14} & 0 \\ k_{21} & k_{22} & k_{23} & 0 & k_{25} \\ k_{31} & k_{32} & k_{34} & 0 & k_{35} \\ k_{41} & k_{42} & k_{43} & 0 & k_{45} \\ k_{51} & k_{52} & k_{53} & 0 & 0 \end{bmatrix}$$

It can also be summarized in terms of transmission as follows (Hartemink et al. 2008):

$$\boldsymbol{K} = \begin{bmatrix} transovarial & transovarial & transovarial & transovarial & 0 \\ cofeeding & cofeeding & cofeeding & 0 & systemic\ (host \rightarrow larvae) \\ cofeeding & cofeeding & cofeeding & 0 & systemic\ (host \rightarrow nymph) \\ cofeeding & cofeeding & cofeeding & 0 & systemic\ (host \rightarrow adult) \\ tick \rightarrow host & tick \rightarrow host & tick \rightarrow host & 0 & 0 \end{bmatrix}$$

The dominant eigenvalue of the NGM, **K**, can be interpreted in a meaningful way both mathematically and biologically. Mathematically, this eigenvalue means that the generations are either growing in size (if it is greater than 1) or decreasing in size (if it is smaller than 1). Biologically, this number can be interpreted as the per-generation growth factor of the infected population of all types-at-birth. Therefore, this eigenvalue is an estimate of R_0 (Hartemink et al. 2008).

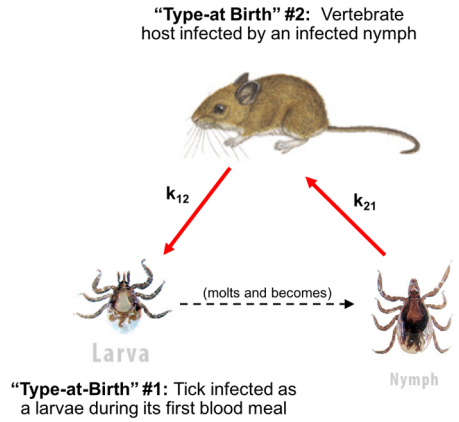

Figure 1. The simplified transmission cycle of *B. burgdorferi*

In order to determine which transmission pathways are most important for different tick-borne disease pathogens, Davis and Bent (2011) identified seven different host-types-at-birth. A loop analysis revealed that for *B. burgdorferi*, transmission is effectively dependent only on the route between susceptible larvae that become infected during their first blood meal and vertebrate hosts infected by nymphal ticks (Davis & Bent 2011). This finding is supported by many other studies in the literature, which indicate that nonsystemic/co-feeding transmission and vertical/transovarial transmission are not important pathways for *B. burgdorferi* in the United States (Spielman et al. 1985; Schoeler & Lane 1993; Gray 1998; Piesman & Gern 2004; Rollend et al. 2013). Therefore, the NGM can be simplified to two types-at-birth, resulting in the following (Dunn 2014):

$$\boldsymbol{K} = \begin{bmatrix} 0 & k_{12} \\ k_{21} & 0 \end{bmatrix} \text{ and } \qquad R_0 = \sqrt{k_{12}k_{21}}$$

where

Host type 1 = tick infected during its first blood meal as a larva

Host type 2 = vertebrate host infected by an infectious nymph

and

k_{12} = Expected # of larvae infected by 1 mouse

k_{21} = Expected # of mice with infected by 1 nymph

$$k_{21} = s_N * q_N * c$$

$$k_{12} = \int_{t=0}^{t=365} a_N(t) \int_{t'=0}^{t'=365-t} \frac{1}{d_L} p(t')\theta^{t'} \overline{Z}_L(t'+t)dt'dt$$

Parameters are defined in Table 1.

This generalization is particularly relevant for the ecology of Lyme disease on Block Island due to the simplified host community for the immature stages of *I. scapularis*. Unlike mainland sites, potential hosts are limited to meadow voles, Norway rats, white-footed mice, and various species of birds. Furthermore, since *P. leucopus* are the most common host, have the highest tick burdens, and are the most competent host for horizontal transmission of *B. burgdorferi*, accounting for *P. leucopus* should

capture the majority of transmission (Piesman & Spielman 1979; Main et al. 1982; Donahue et al. 1987; Mather et al. 1989).

CO-AGGREGATION AND THE R_0 MODEL

Despite this simplification, it may still be important to account for co-aggregation of larval and nymphal ticks on the same mice. That is, if particular mice provide the majority of nymphal blood meals, then they have a higher probability of becoming infected. If the majority of larval ticks also feed on these same mice, then the rate of horizontal transmission would be greater. Co-aggregation of the same life stage on the same mice is not important because, in the absence of transovarial transmission, larvae cannot infect other larvae. Moreover, if infected nymphs infect other susceptible nymphs, it no longer matters for disease transmission because adults feed mainly on *O. virginianus* and do not contribute significantly to transmission of the pathogen to humans. The mice with both high nymphal and larval burdens are "super-spreader" mice, which would be responsible for a higher number of secondary infections than an average mouse. In order to account for co-aggregation of the two life stages, the model can be expanded to four types-at-birth (Figure 2, Dunn 2014). Therefore, the revised R_0 model is given as follows (Dunn 2014):

$$R_0 = \sqrt{k_{12}k_{21} + k_{13}k_{31}}$$

where

k_{12} = Expected # of larvae infected by 1 mouse with high tick burdens

k_{21} = Expected # of mice with high tick burdens infected by 1 nymph

k_{13} = Expected # of larvae infected by 1 mouse with low tick burdens

k_{31} = Expected # of mice with low tick burdens infected by 1 nymph

and are given by the following equations (see also Table 1):

$$k_{21} = m * s_N * q_N * c$$

$$k_{31} = (1 - m) * s_N * q_N * c$$

$$k_{12} = \int_{t=0}^{t=365} a_{N,high}(t) \int_{t'=0}^{t'=365-t} \frac{1}{d_L} p(t') \theta^{t'} \overline{Z}_{L,high}(t' + t) dt' dt$$

$$k_{13} = \int_{t=0}^{t=365} a_{N,low}(t) \int_{t'=0}^{t'=365-t} \frac{1}{d_L} p(t') \theta^{t'} \overline{Z}_{L,low}(t' + t) dt' dt$$

For estimation of the parameter values, please see Appendices C and D.

Table 1. *A description of parameters for the R_0 model*

Parameter	**Description**
t	time of infection of a mouse
t'	number of days since infection in a single mouse
m	the proportion of ticks feeding on high tick burden mice rather than low tick burden mice (degree of co-aggregation)
s_N	proportion of fed larvae that survive to nymphs
q_N	probability of transmission from infected nymphs to mice
c	proportion of nymphs that successfully find a mammal host (*P. leucopus*)
$a_N(t)$	proportion of host seeking nymphs that emerge and feed at time t (with co-aggregation: activity differs for high and low burden mice)
$p(t')$	infectivity of hosts as a function of days post infection
$\theta^{t'}$	mouse survival (the proportion of P. leucopus t' days after infection)
$\overline{Z}_L(t'+t)$	expected larval burden on mice (with co-aggregation: high or low burden mice)

Figure 2. The co-aggregated transmission cycle for *B. burgdorferi*

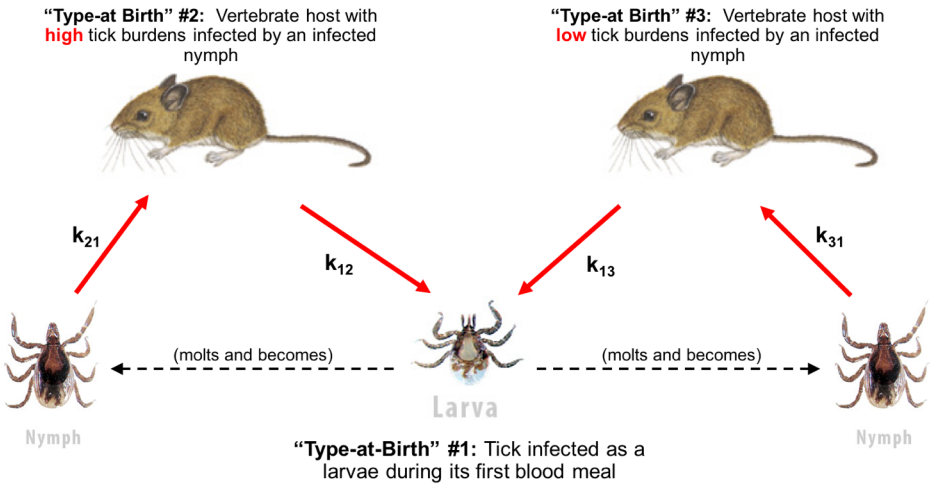

APPENDIX C.

Estimation of Expected Tick Burdens

METHODOLOGY

In order to estimate the number of ticks on a mammal host on any given day, *t*, of the year, the expected (mean) tick burden was modelled from the mammal trapping field data. The curves were fit to the data in the manner developed by Brunner and Ostfeld (2008) and Dunn et al. (2013). The expected nymphal burden, $\bar{Z}_N(t)$, can be described by a right shifted lognormal curve, and the expected larval burden, $\bar{Z}_L(t)$, can be described by an earlier right shifted normal curve for spring activity and a later log normal curve for fall activity (Brunner and Ostfeld 2008, Figure 1}.

The equations are given as follows:

$$\bar{Z}_N(t) = \begin{cases} 0 & , if\ t < \tau_N \\ H_N * e^{-0.5\left(\ln\left(\frac{[day\ of\ year - \tau_N]/\mu_N}{\sigma_N}\right)\right)^2} & , if\ t \geq \tau_N \end{cases}$$

$$\bar{Z}_L(t) = \begin{cases} 0 & , if\ t < \tau_E \\ H_E * e^{-0.5\left(\frac{(day\ of\ year - \tau_E)/\mu_E}{\sigma_E}\right)^2} & , if\ t \geq \tau_E \\ H_L * e^{-0.5\left(\ln\left(\frac{[day\ of\ year - \tau_L]/\mu_L}{\sigma_L}\right)\right)^2} & , if\ t \geq \tau_L \end{cases}$$

where

H = height of the peak expected burden

τ = number of days to the beginning of tick activity (shift)

μ = shape parameter defining the number days from the beginning of tick activity until the peak

σ = shape parameter determining the duration and slope of tick activity

The curves were fitted by a maximum likelihood estimation method for overdispersed, zero-inflated data with a negative binomial distribution within a single trapping day (Dunn 2014). For paired tick count data, x_i, on a given day, t_i, with mean $\mu(t_i)$ and dispersion parameter α, the likelihood equation is given by

$$\mathcal{L}\left(\mu, \alpha \middle| data[(t_1, x_1), \ldots, (t_n, x_n)]\right) = \prod_{i=1}^{n} \frac{\Gamma(x_i + \alpha^{-1})}{x_i!\,\Gamma(\alpha^{-1})} \left(\frac{\alpha^{-1}}{\alpha + \mu(t_i)}\right)^{\alpha^{-1}} \left(\frac{\mu(t_i)}{\alpha^{-1} + \mu(t_i)}\right)^{x_i}$$

This assumes that α, the dispersion parameter, stays constant throughout the year while the mean $\mu(t_i)$ varies and is described by $\bar{Z}_N(t)$ or $\bar{Z}_L(t)$ for nymphal or larval burdens respectively.

Figure 1. The models to describe the expected (a) nymphal and (b) larval tick burdens on a mouse during any given day of the year. From Brunner and Ostfeld (2008), Figure 1, page 2262. The "shift" is given by τ in the equations above.

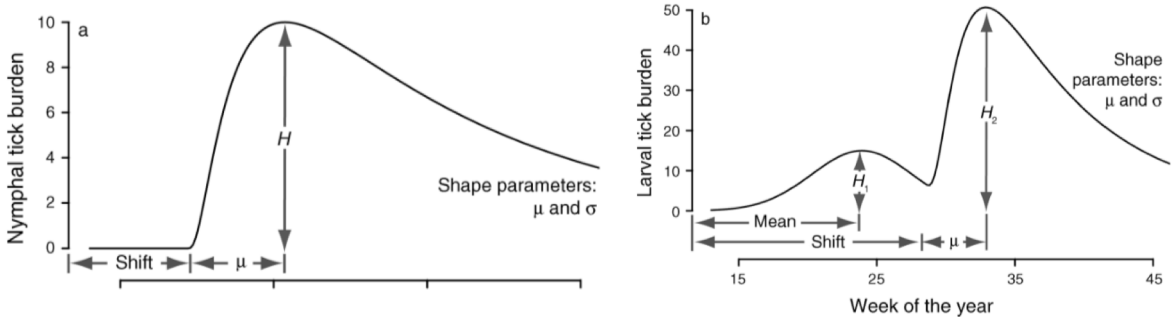

The field data was not always best modelled by a lognormal (for nymphs) or normal-lognormal (for larvae) curve. Therefore, the curves were adjusted to allow for the best possible fit for the mean tick burdens on mice. Details on the equations and parameter values for all model scenarios are described in the following two sections.

Nymphal Burdens

Mainland 2014

Overall and co-aggregated nymphal means for the Connecticut site were all modelled by lognormal curves. The parameter values and curves are shown in table 1 and figures 2-4.

Table 1. *Parameter estimates for the mean nymphal burdens for 2014 Connecticut field data*

Data Set	Type of Curve	Height	τ	μ	σ	α
Mainland Overall	Log Normal	1.3	103.6	58.2	0.4	0.5
Mainland High Burden	Log Normal	2.2	132.3	18.6	0.9	0.2
Mainland Low Burden	Log Normal	0.4	133.3	8.7	2.4	0.0

Figure 2. The expected nymphal burden plotted against the individual nymphal burden observations and average nymphal burden observations for all Connecticut 2014 mice.

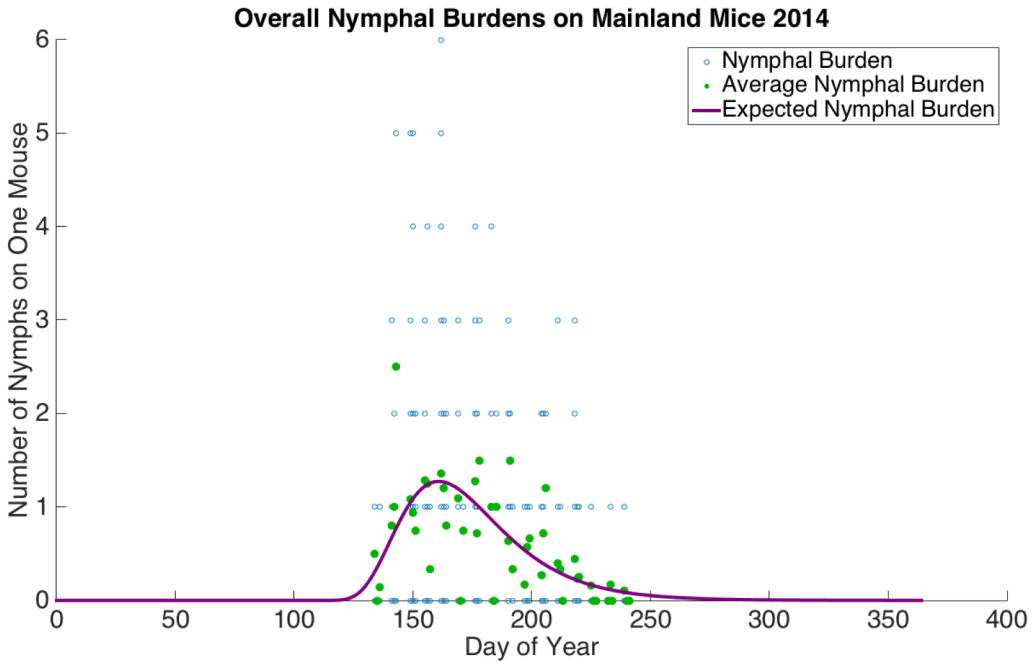

Figure 3. The expected nymphal burden plotted against the individual nymphal burden observations and average nymphal burden observations for high burden ("super-spreader") Connecticut 2014 mice.

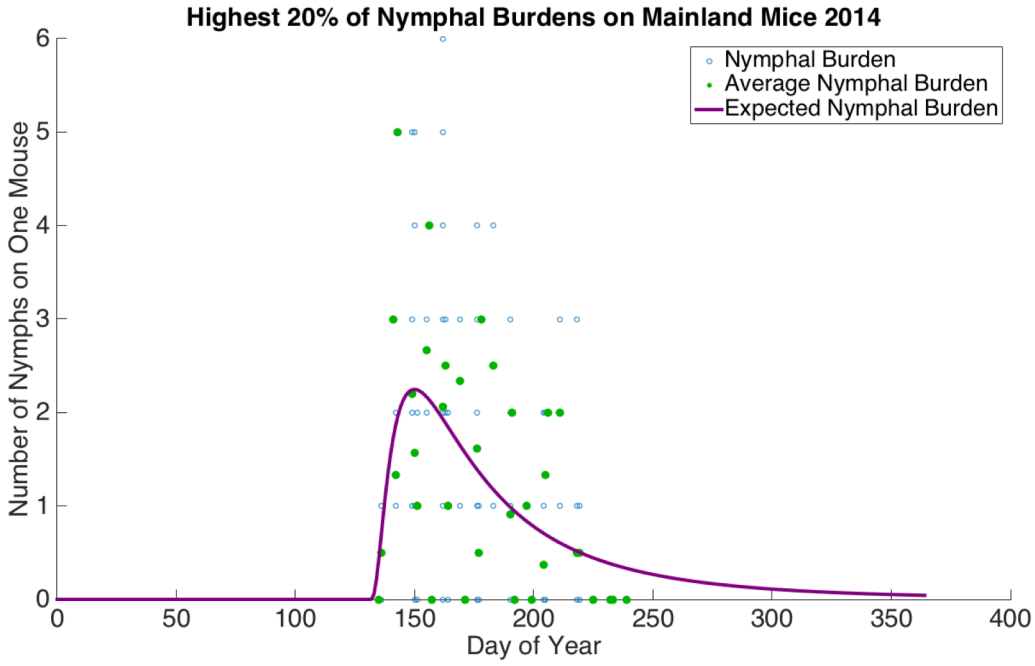

Figure 4. The expected nymphal burden plotted against the individual nymphal burden observations and average nymphal burden observations for low burden Connecticut 2014 mice.

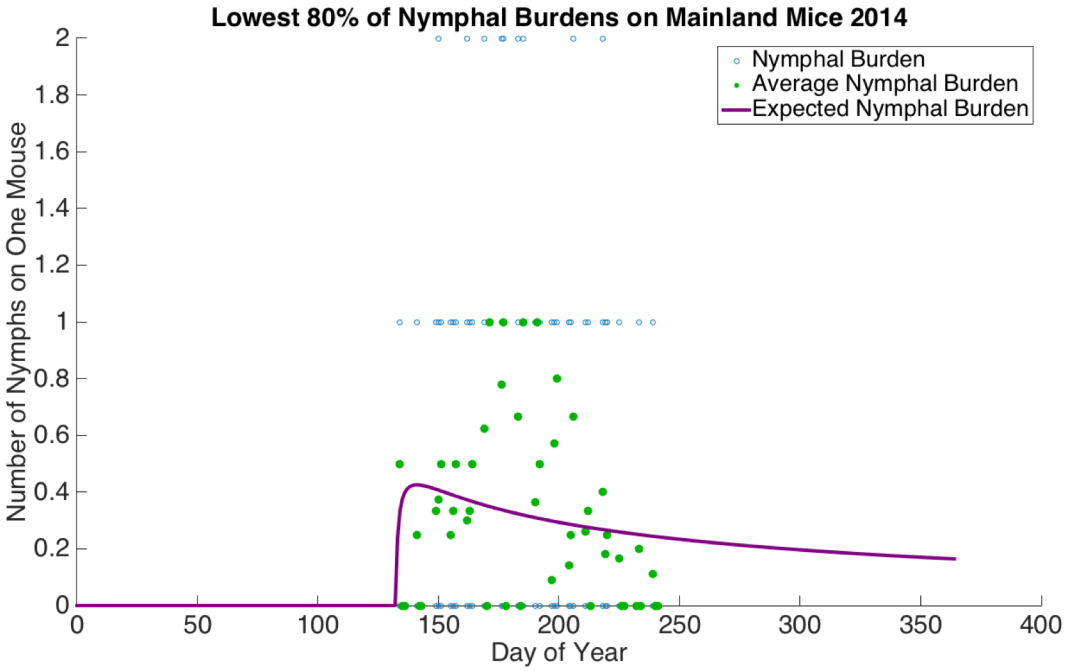

Block Island 2014

Overall and co-aggregated nymphal means for the Block Island site in 2014 were modelled by normal and lognormal curves. The parameter values and curves are shown in table 2 and figures 5-7.

Table 2. *Parameter estimates for the mean nymphal burdens for 2014 Block Island field data*

Data Set	**Type of Curve**	**Height**	**τ**	**μ**	**σ**	**α**
Island 2014 Overall	Normal	7.8	142.6	19.7	24.5	0.8
Island 2014 High Burden	Log Normal	14.7	135.5	19.0	0.7	0.5
Island 2014 Low Burden	Normal	4.6	138.3	23.8	25.8	0.4

Figure 5. The expected nymphal burden plotted against the individual nymphal burden observations and average nymphal burden observations for all Block Island 2014 mice.

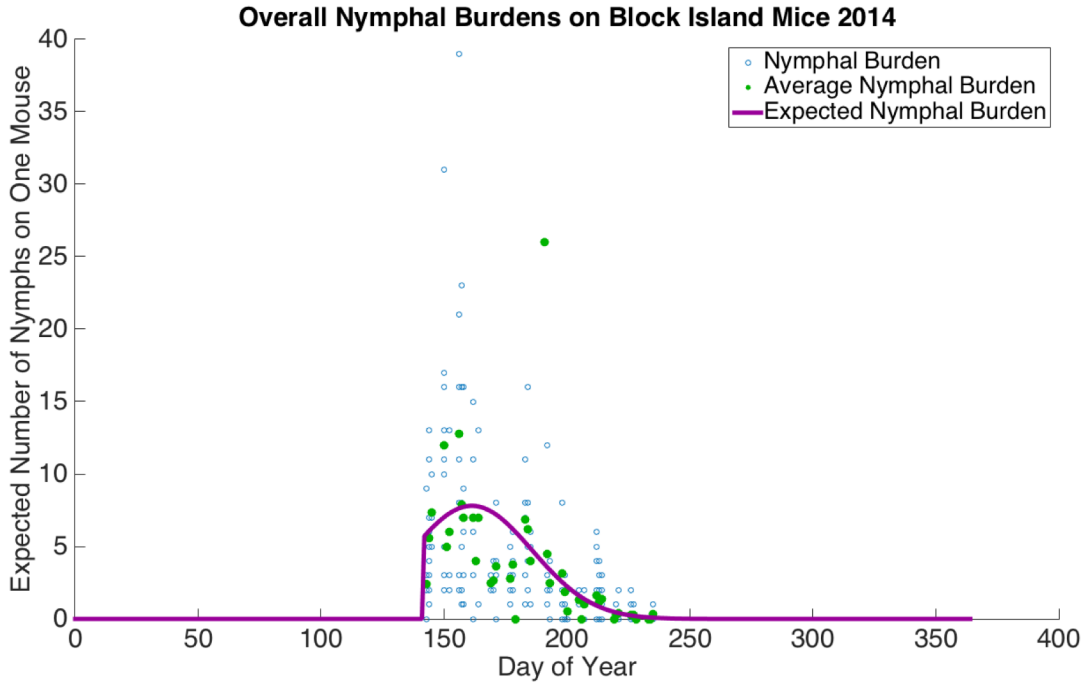

Figure 6. The expected nymphal burden plotted against the individual nymphal burden observations and average nymphal burden observations for high burden ("super-spreader") Block Island 2014 mice.

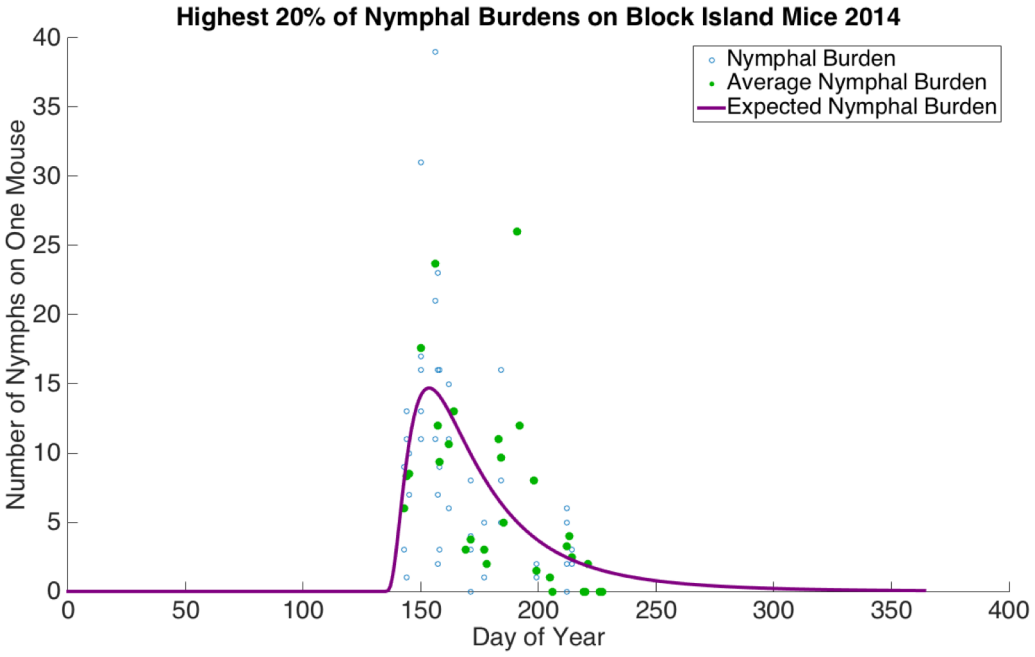

Figure 7. The expected nymphal burden plotted against the individual nymphal burden observations and average nymphal burden observations for low burden Block Island 2014 mice.

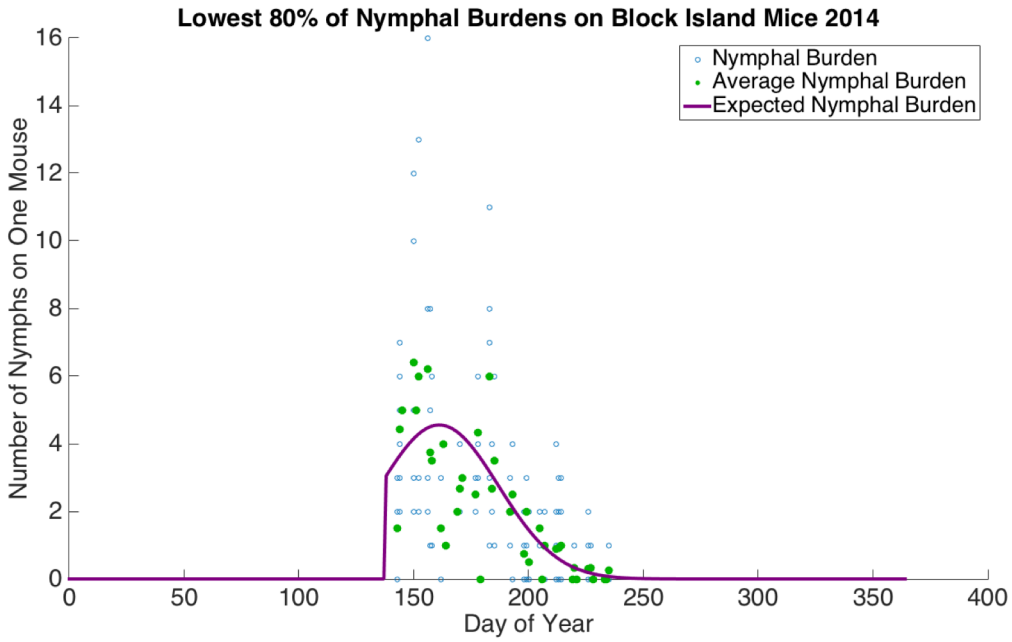

Block Island 2013

Overall and co-aggregated nymphal means for the Block Island site in 2013 were modelled by normal curves. The parameter values and curves are shown in table 3 and figures 8 - 10.

Table 3. *Parameter estimates for the mean nymphal burdens for 2014 Block Island field data*

Data Set	**Type of Curve**	**Height**	**τ**	**μ**	**σ**	**α**
Island 2013 Overall	Normal	4.6	140.1	24.8	21.8	0.7
Island 2013 High Burden	Normal	6.7	133.6	33.5	20.6	0.8
Island 2013 Low Burden	Normal	2.9	134.2	27.2	25.2	0.2

Figure 8. The expected nymphal burden plotted against the individual nymphal burden observations and average nymphal burden observations for all Block Island 2013 mice.

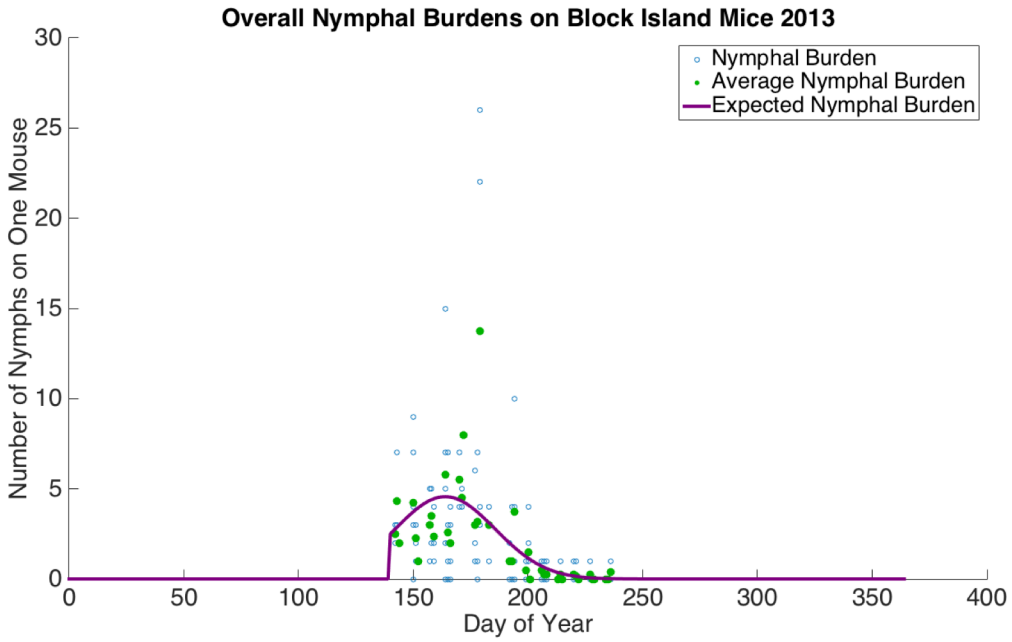

Figure 9. The expected nymphal burden plotted against the individual nymphal burden observations and average nymphal burden observations for high burden ("super-spreader") Block Island 2013 mice.

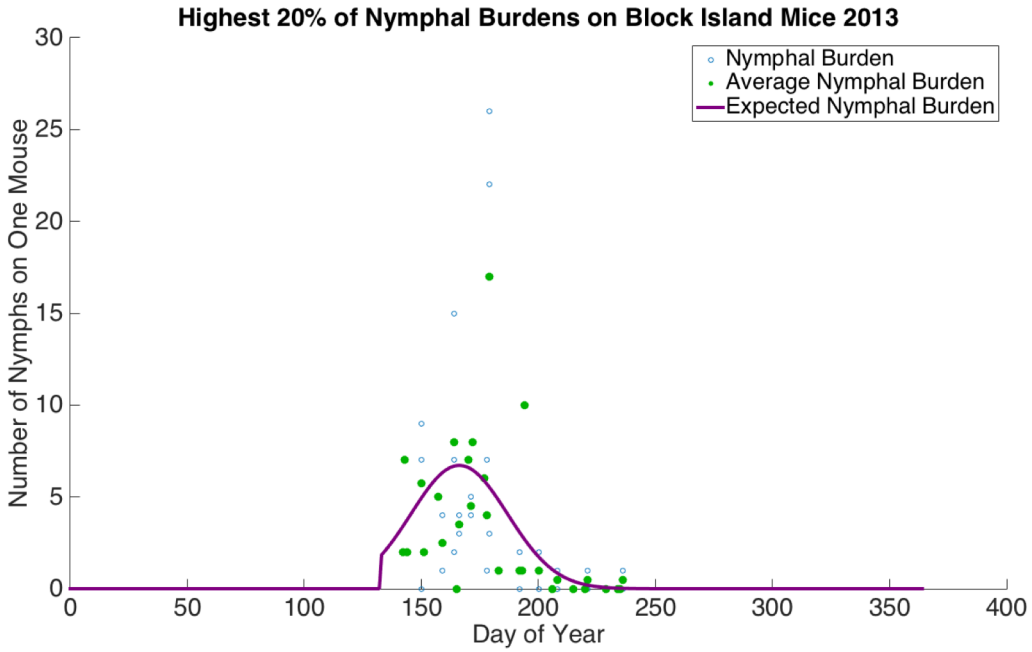

Figure 10. The expected nymphal burden plotted against the individual nymphal burden observations and average nymphal burden observations for low burden Block Island 2013 mice.

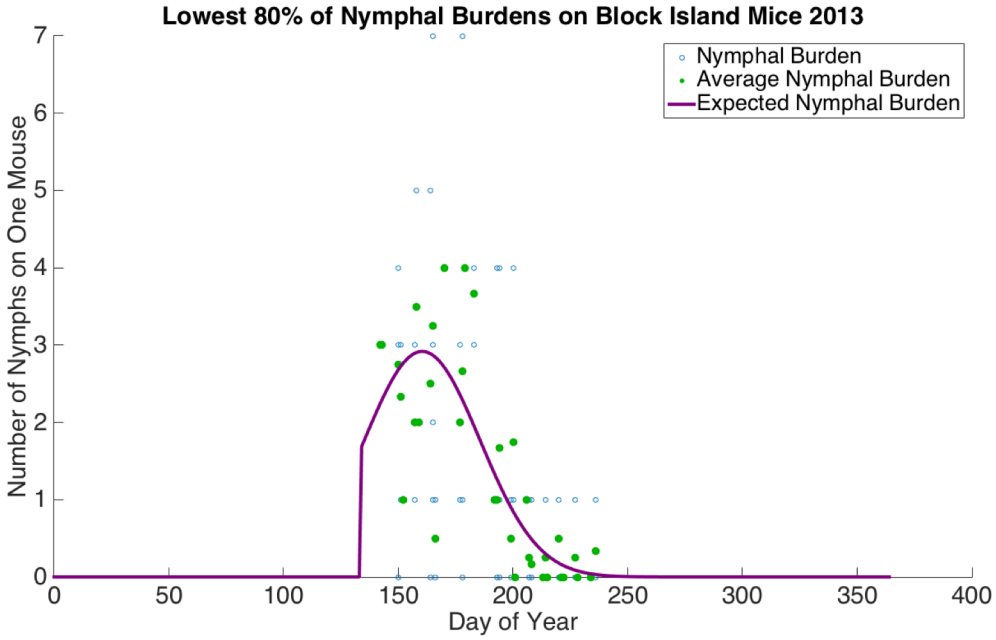

LARVAL BURDENS

Mainland 2014

Overall and co-aggregated larval means for the Connecticut site were all modelled by lognormal curves. The parameter values and curves are shown in table 4 and figures 11-13.

Table 4. *Parameter estimates for the mean larval burdens for 2014 Connecticut field data*

Data Set	Curve	Spring Height	Spring τ	Spring μ	Spring σ	Fall Height	Fall τ	Fall μ	Fall σ	α
Mainland Overall	Log Normal Normal	2.5	129.9	18.6	0.8	13.3	200.8	27.8	15.4	0.7
Mainland High Burden	Log Normal Normal	2.1	135.1	15.4	0.8	18.3	199.0	29.1	16.3	0.5
Mainland Low Burden	Log Normal Normal	2.5	131.1	16.9	0.9	7.6	190.0	37.9	13.7	0.5

Figure 11. The expected larval burden plotted against the individual larval burden observations and average larval burden observations for all Mainland 2014 mice.

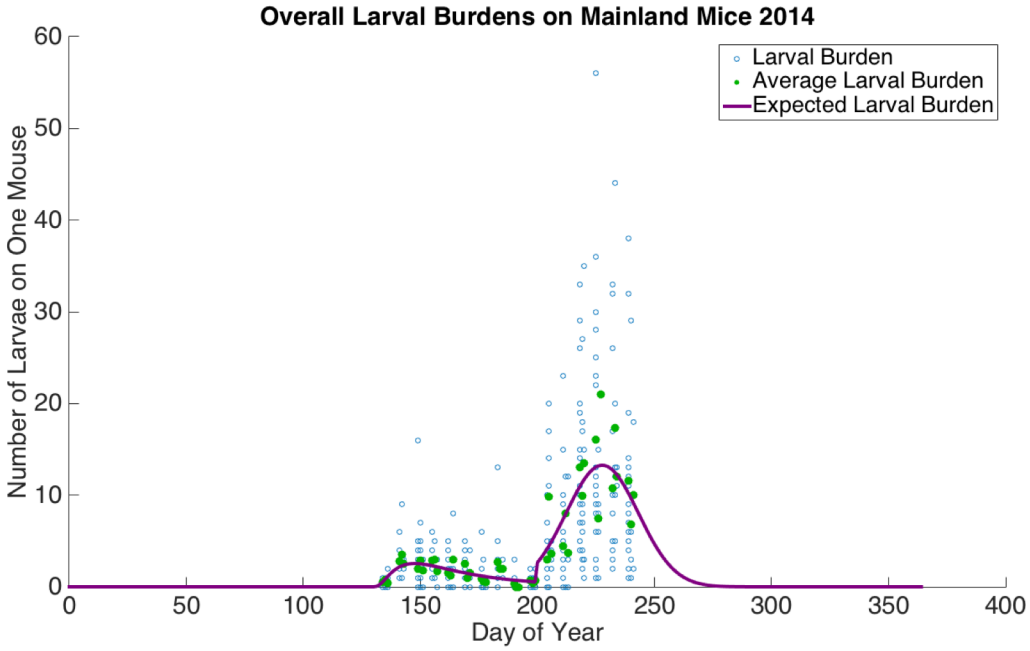

Figure 12. The expected larval burden plotted against the individual larval burden observations and average larval burden observations for high burden ("super-spreader") Mainland 2014 mice.

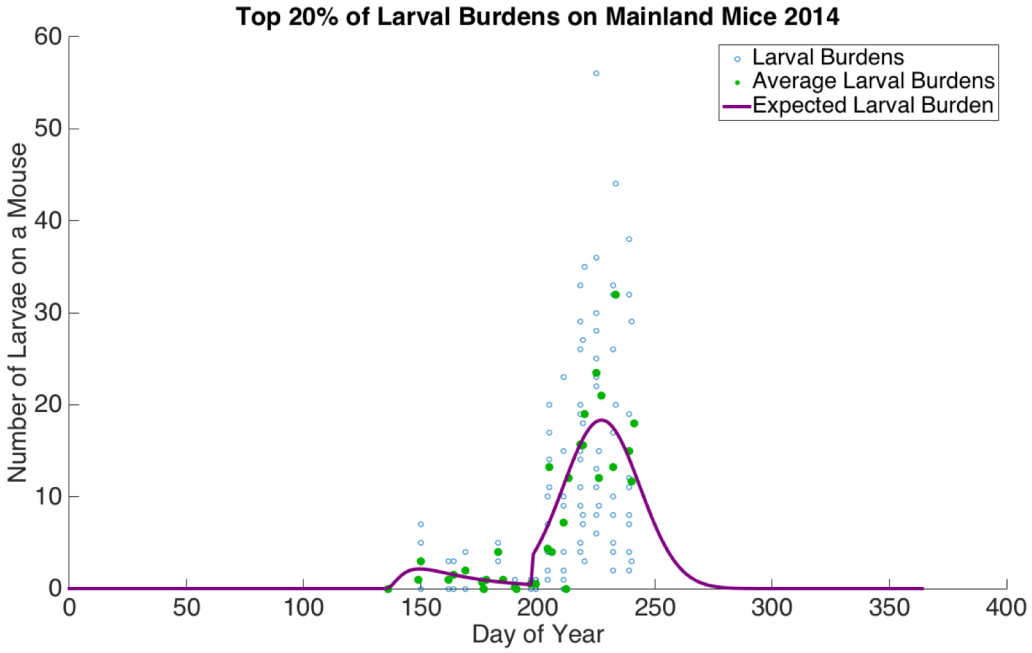

Figure 13. The expected larval burden plotted against the individual larval burden observations and average larval burden observations for low burden Mainland 2014 mice.

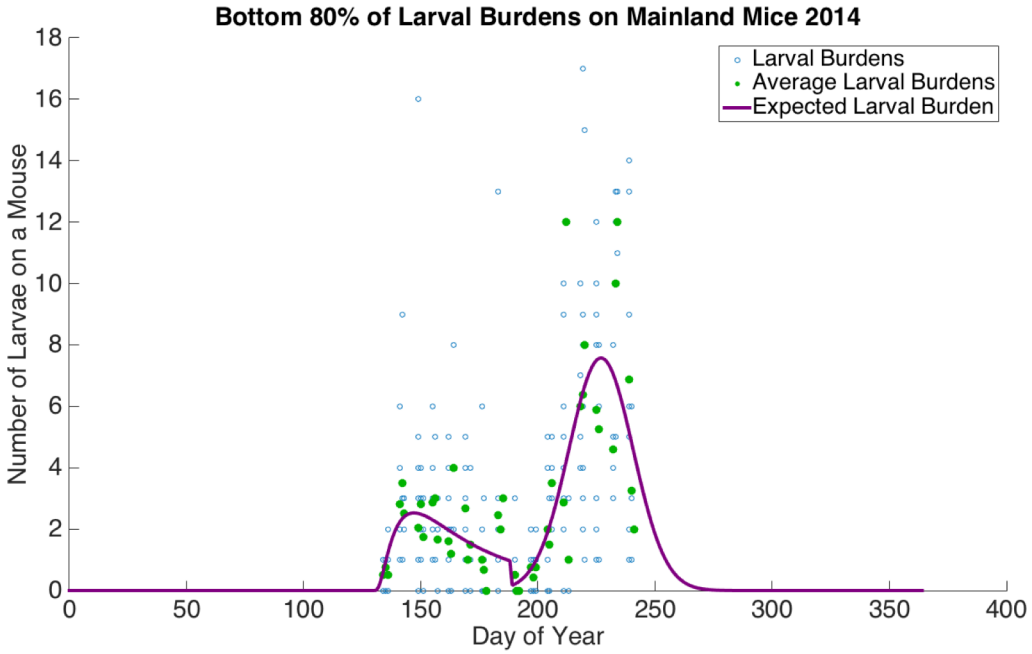

Block Island 2014

Overall and co-aggregated larval means for the Block Island 2014 site were modelled by uniform and lognormal curves. The parameter values and curves are shown in table 5 and figures 14-16.

Table 5. *Parameter estimates for the mean larval burdens for 2014 Block Island field data*

Data Set	Curve	Spring Height	Spring τ	Spring μ	Spring σ	Fall Height	Fall τ	Fall μ	Fall σ	α
Island 2014 Overall	Uniform Log Normal	2.1	141.7	---	---	61.9	203.3	11.9	0.8	0.9
Island 2014 High Burden	Log Normal Log Normal	3.9	144.0	0.3	3.4	122.7	183.0	34.2	0.3	0.4
Island 2014 Low Burden	Linear Normal	---	143.0	---	---	24.6	207.0	13.7	21.3	0.6

Figure 14. The expected larval burden plotted against the individual larval burden observations and average larval burden observations for all Block Island 2014 mice.

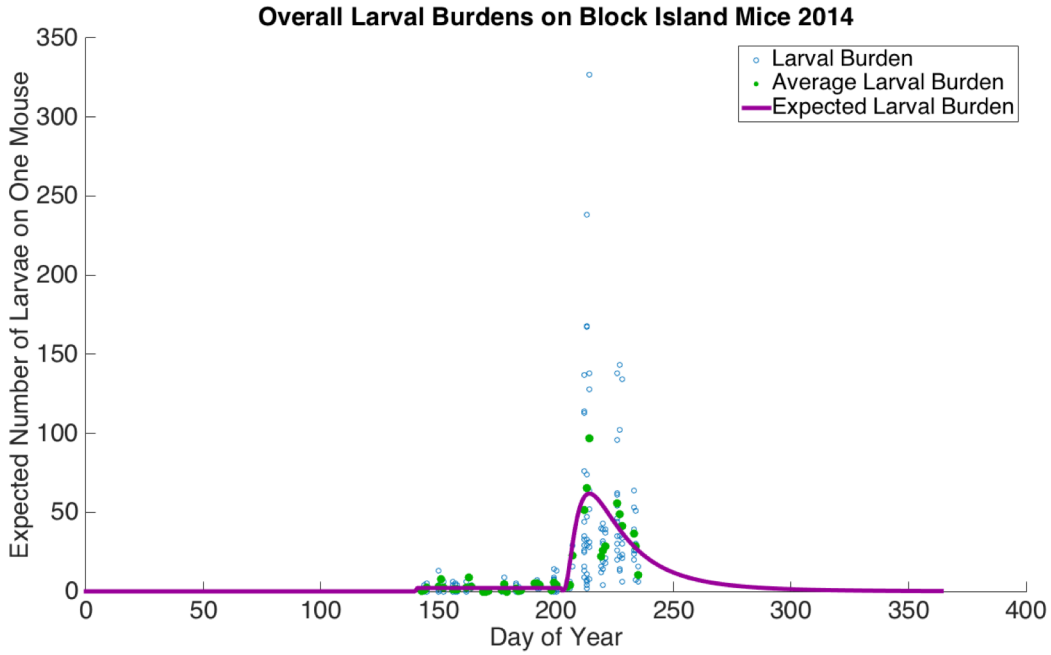

Figure 15. The expected larval burden plotted against the individual larval burden observations and average larval burden observations for high burden ("super-spreader") Block Island 2014 mice.

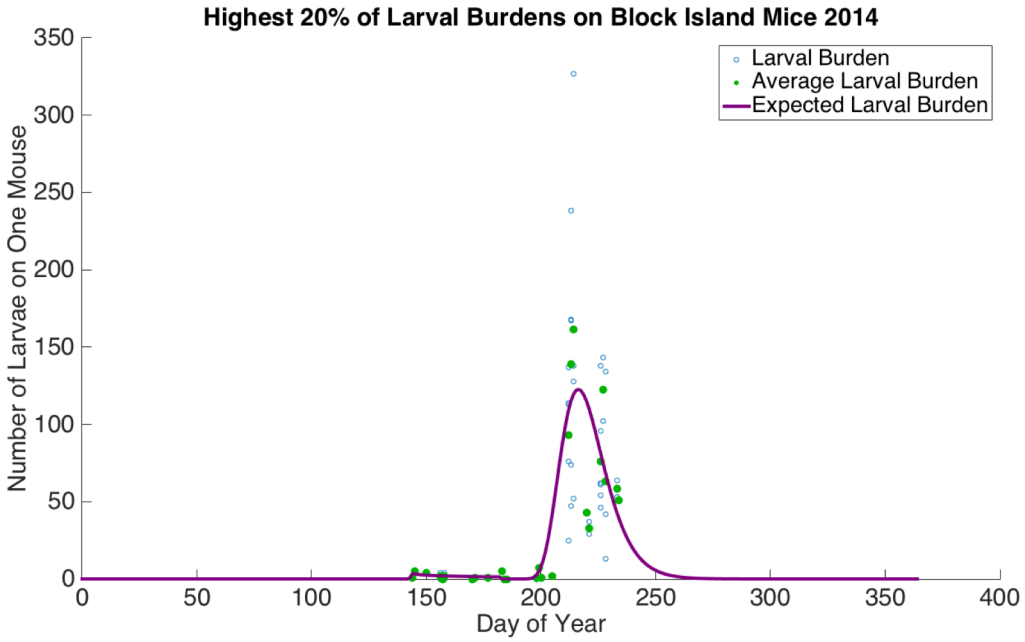

Figure 16. The expected larval burden plotted against the individual larval burden observations and average larval burden observations for low burden Block Island 2014 mice.

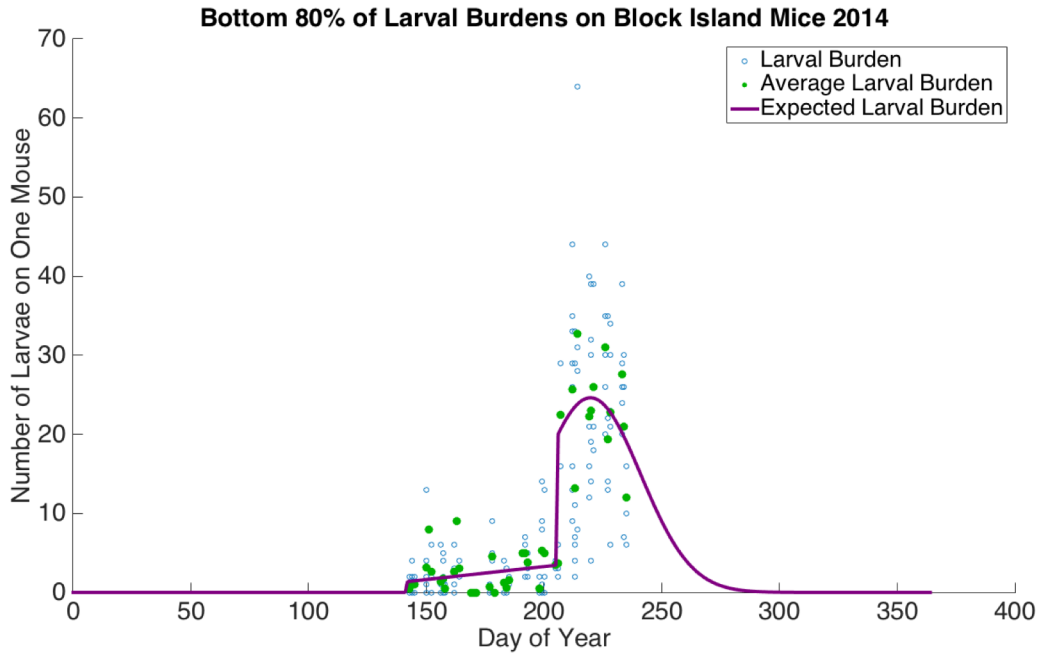

Block Island 2013

Overall and co-aggregated larval means for the Block Island 2013 site were modelled by uniform and normal curves. The parameter values and curves are shown in table 6 and figures 17-19.

Table 6. *Parameter estimates for the mean larval burdens for 2013 Block Island field data*

Data Set	Curve	Spring Height	Spring τ	Fall Height	Fall τ	Fall μ	Fall σ	α
Island 2013 Overall	Uniform Normal	0.3	142.6	48.5	182.5	27.9	11.7	0.6
Island 2013 High Burden	Uniform Normal	0.4	143.0	58.1	193.0	26.2	12.0	0.6
Island 2013 Low Burden	Uniform Normal	0.3	140.2	30.8	192.6	30.4	14.6	0.5

Figure 17. The expected larval burden plotted against the individual larval burden observations and average larval burden observations for all Block Island 2013 mice.

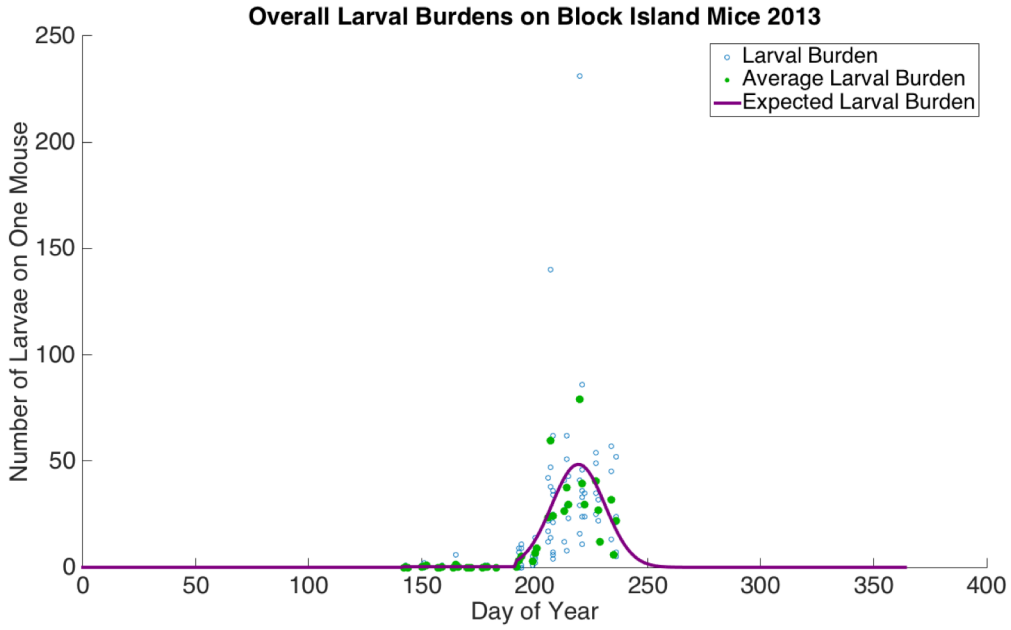

Figure 18. The expected larval burden plotted against the individual larval burden observations and average larval burden observations for high burden ("super-spreader") Block Island 2013 mice.

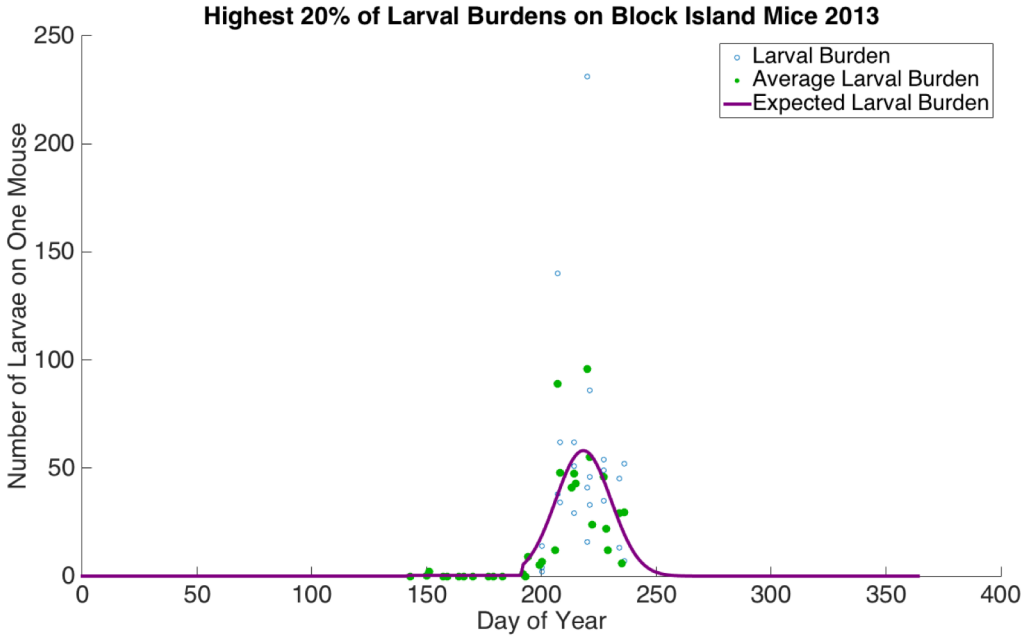

Figure 19. The expected larval burden plotted against the individual larval burden observations and average larval burden observations for low burden Block Island 2013 mice.

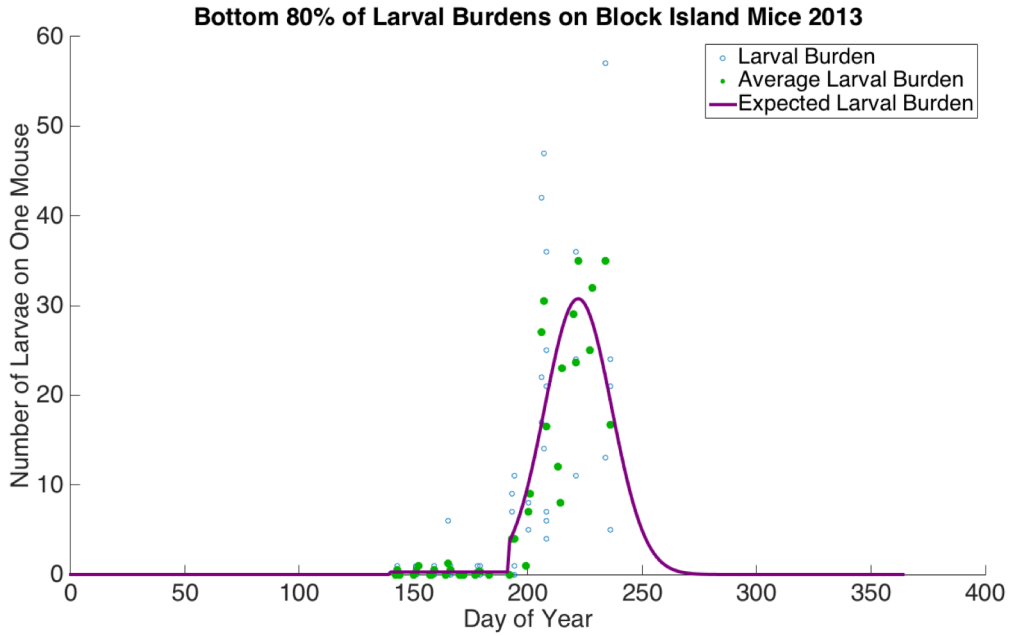

APPENDIX D.

Estimation of Model Parameters and Median Values from Wilcoxon Rank Sum Tests

INFECTIVITY OF HOSTS AS A FUNCTION OF DAYS POST INFECTION, P(T')

A mouse infected with *B. burgdorferi* will be infectious to nymphs at different levels throughout the duration of infection. The data used to estimate the infectivity of *P. leucopus* as a function of days post infection was from a transmission experiment conducted at the Diuk-Wasser laboratory (States, unpublished data). For eight different time points spanning a period of 100 days, 100 uninfected larvae were allowed to feed on *P. leucopus* hosts infected with *B. burgdorferi* strain ospC type C. Larvae were collected and allowed to molt into nymphs, which were then tested for infection. From a grand total of 215 molted and tested nymphs, the proportion of infected ticks from each feeding time point was recorded. The mean infection prevalence curves were estimated via a log-normal distribution and fit using the same methodology as the tick burden curves (Table 1, Figure 1, Appendix C).

$$p(t') = H * e^{-0.5\left(ln\left(\frac{[t']/\mu}{\sigma}\right)\right)^2}$$

Table 1. *The parameter estimates for the log-normal infection curve*

***B. burgdorferi* Strain**	**Height**	**μ**	**σ**	**α**
ospC Type C	1	23.3	1.1	0.0016

Figure 1. *The mean infectivity of mice to larvae as a function of days post infection, estimated via proportion of molted nymphs infected after feeding on mammal hosts infected by* B. burgdorferi *ospC type C*

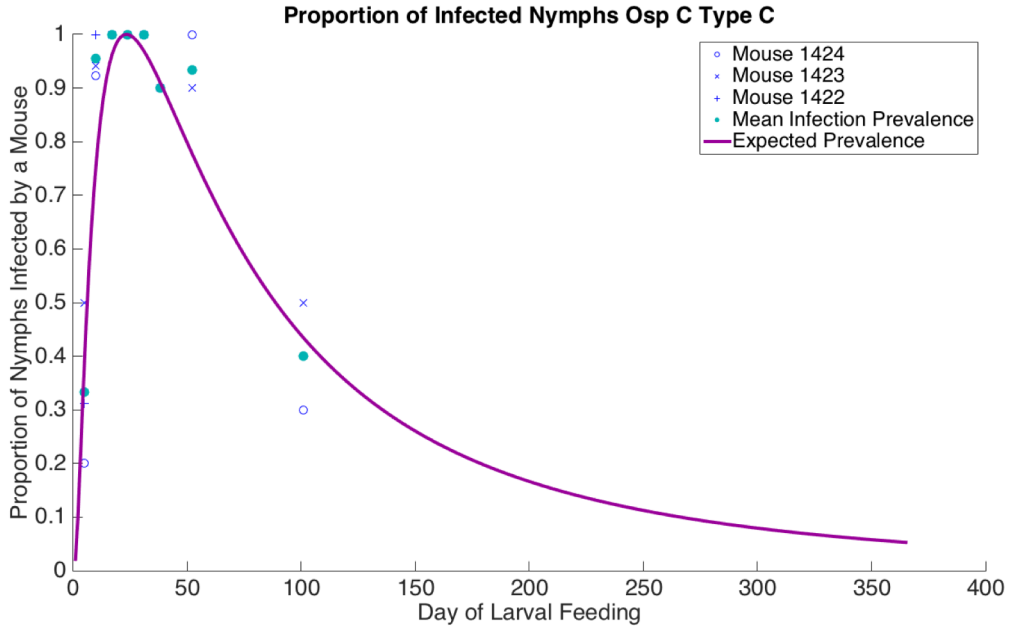

Proportion of Host-Seeking Nymphs that Emerge and Feed at Time t, $a_N(t)$

The proportion of host-seeking nymphs on day t is calculated using the nymphal burden curves and the following equation (see Appendix C for nymphal burden curve estimation):

$$a_N(t) = \frac{\bar{Z}_N(t)}{\int_0^{365} \bar{Z}_N(t)}$$

Survival of White Footed Mice Post Infection, θ

The survival of white-footed mice was estimated from the field data via Program MARK. If the survival estimates differed for males and females, then the average overall survival was weighted by sex (Table 2). The survivorship estimates are only valid for the duration of the field season (~May – August). However, these survivorship estimates should be sufficient for the purposes of the R_0 model because infection calculations are limited by the duration of tick activity and the infectivity of mice to nymphs (Appendix C; Appendix D, figure 1).

Table 2. Demographics and Survivorship of *P. leucopus* estimated from field data.

Site	% Female	Female Survivorship	Male Survivorship	Overall Survivorship
Mainland 2014	39%	0.642	0.634	**0.637**
Island 2014	36%	0.894	0.827	**0.851**
Island 2013	51%	0.771	0.760	**0.765**

Larval Survival and Host-Seeking Success, c^*s_N

The product of the survival of fed larvae in year 1 to questing nymphs in year 2, s_N, and the probability that a questing nymph will find a competent host (in this case, *P. leucopus*), c, can be estimated with two consecutive years of field data. If one makes the assumption that the nymphs feeding on mice in year 2 are the same ticks as the larvae that fed on mice in year 1, then c^*s_N can be estimated by the following equation:

$$c * s_N = \frac{\int_0^{365} \bar{Z}_N(t) \text{ from year 2}}{\int_0^{365} \bar{Z}_L(t) \text{ from year 1}}$$

Since there are two consecutive years of field data for Block Island (2013 and 2014), this product was calculated and used in both the 2013 and 2014 Island R_0 scenarios.

Remaining Parameters

All remaining parameters were estimated from values found in the literature. These parameters are days of larval attachment to a host, d_L, and probability of pathogen transmission from a nymph to a host, q_N. For the mainland 2014 model, parameter values for c and s_N were also taken from the literature.

Empirical Evidence for Co-Aggregation - Medians

High tick burden mice were determined by sorting according to *larval* burdens and examining the relationship between the nymphal and larval burdens from the top 10%, 20%, 30% or 40% mice compared to the bottom y% (top two rows in Table 3 and top three rows in Table 4). Since the highest larval burdens did not always co-occur with the highest nymphal burdens, a second round of tests was

also performed by comparing the nymphal burdens on mice sorted according to high vs. low *nymphal* burdens (last row in Tables 3 and 4).

Since these data were not normally distributed and the subgroup sample sizes were small, Wilcoxon Rank Sum tests were performed to determine if the median tick burden of "high burden" mice was significantly higher than the median tick burden of "low burden" mice. A two-way test was used in order to generate conservative p-values, and medians were compared in order to confirm that the "high burden" mice did indeed have a greater number of ticks than "low burden" mice (Tables 3 and 4). For the Mainland 2014 data set, the median values for nymphal burden on mice sorted according to larval burdens were not informative, so the mean values are also reported (rows 2 and 3 of Table 4). "High" burden medians are italicized (ranging from 5 to 40% of the total mouse population).

Table 3. Median tick burdens of subpopulations for Block Island 2014 mice

	90%	**80%**	**70%**	**60%**	***40%***	***30%***	***20%***	***10%***
Larvae	35	35	32	26.5	*116*	*149*	*192*	*270*
Nymphs	12	12.5	13	8	*21*	*16.5*	*21*	*22*
By Nymphs	11	8	7	6.5	*22*	*25.5*	*28*	*40*

Table 4. Median (and mean) tick burdens of subpopulations of Mainland 2014 mice

	95%	**90%**	**80%**	**70%**	**60%**	***40%***	***30%***	***20%***	***10%***	***5%***
Larvae	4	4	3	3	2	*16.5*	*20*	*32*	*37*	*47*
Nymphs	1	1	1	1	0	*1*	*1*	*1*	*1*	*1*
Nymphs Mean	1.5	1.6	1.4	1.2	1.0	*2.3*	*2.3*	*2.1*	*1.8*	*2.1*
By Nymphs	1	1	0	0	0	*3*	*3*	*5*	*6*	*7*

APPENDIX E.

Full Results from the Sensitivity/Elasticity Analysis

A local sensitivity analysis was performed by varying one parameter value while keeping all other parameters constant. However, since sensitivity values are influenced by the unit values of the parameter in question, the elasticity values can be more useful for comparison. Elasticity is a measure of the relative change in R_0 for a proportional change in one parameter value.

All sensitivity/elasticity analyses were performed on the simple case R_0 model, with the exception of the m parameter (Tables 1-4). The m parameter was the only one investigated for the co-aggregation R_0 model.

Table 1. The results for the elasticity analysis on the Connecticut 2014 Scenario

Mainland 2014	**Point Estimate**	**Range**	**Sensitivity**	**Elasticity**
C^*S_n	0.2	0.1 - 0.3	3.74	**0.37**
$\theta^{t'}$	0.64	0.55 - 0.75	1.13	**0.46**
Nymphal Height	1.27	1 - 4	0.00	0.00
Nymphal Sigma	0.37	0.2 – 0.6	-0.21	-0.03
Spring Larval Height	2.55	1 - 3	0.18	**0.15**
Spring Larval Sigma	0.75	0.5 – 1.0	0.07	0.02
Fall Larval Height	13.26	10 – 20	0.02	**0.16**
Fall Larval Sigma	15.44	10 – 20	0.00	0.00
m	0.8	0.7 - 0.9	0.75	**0.40**

Table 2. The results for the elasticity analysis on the Block Island 2014 Scenario

Island 2014	**Point Estimate**	**Range**	**Sensitivity**	**Elasticity**
C^*S_n	0.27	0.15 – 0.35	23.56	**0.41**
$\theta^{t'}$	0.85	0.75 – 0.95	6.68	**0.47**
Nymphal Height	7.81	5 – 10	0.00	0.00
Nymphal Sigma	24.51	20 – 30	-0.02	-0.04
Spring Larval Height	2.13	1 - 3	0.10	0.01
Fall Larval Height	61.88	50 – 70	0.09	**0.44**
Fall Larval Sigma	0.76	0.5 – 1.0	2.03	0.10
m	0.8	0.7 – 0.9	5.90	**0.40**

Table 3. The results for the elasticity analysis on the Block Island 2013 Scenario

Island 2013	Point Estimate	Range	Sensitivity	Elasticity
C^*S_n	0.27	0.15 – 0.35	4.35	**0.40**
$\theta^{\prime}$	0.77	0.67 – 0.87	1.43	**0.47**
Nymphal Height	4.57	2 – 7	0.00	0.00
Nymphal Sigma	21.81	15 – 25	0.15	**1.84**
Spring Larval Height	0.27	0 – 1	0.33	0
Fall Larval Height	48.47	40 – 60	0.02	**0.41**
Fall Larval Sigma	11.74	9 – 15	0.17	**0.88**
m	0.8	0.7 – 0.9	0.84	**0.12**

Table 4. The results for the elasticity analysis on the Block Island 2014 Scenario with no Spring Larval Peak

Island 2014 (nS)	Point Estimate	Range	Sensitivity	Elasticity
C^*S_n	0.27	0.15 – 0.35	23.14	**0.41**
$\theta^{\prime}$	0.85	0.75 – 0.95	6.57	**0.47**
Nymphal Height	7.81	5 – 10	0.00	0.00
Nymphal Sigma	24.51	20 – 30	-0.02	-0.03
Fall Larval Height	61.88	50 – 70	0.09	**0.46**
Fall Larval Sigma	0.76	0.5 – 1.0	2.06	0.10
m	0.8	0.7 – 0.9	6.30	**0.43**

The effect of the full range of possible m values on the R_0 estimate was determined for all four scenarios (Figures 1-4). As predicted by the elasticity analysis, increasing m results in an increasing R_0 for all models, and the relationship was strongest for the Mainland 2014 and both Block Island 2014 scenarios. The Block Island 2013 scenario was least sensitive, showing a roughly linear relationship (R_0 changing by a total of ~1 as m was varied from 0 to 1).

Figure 1. R_0 as a function of the degree of co-aggregation for the Mainland 2014 scenario

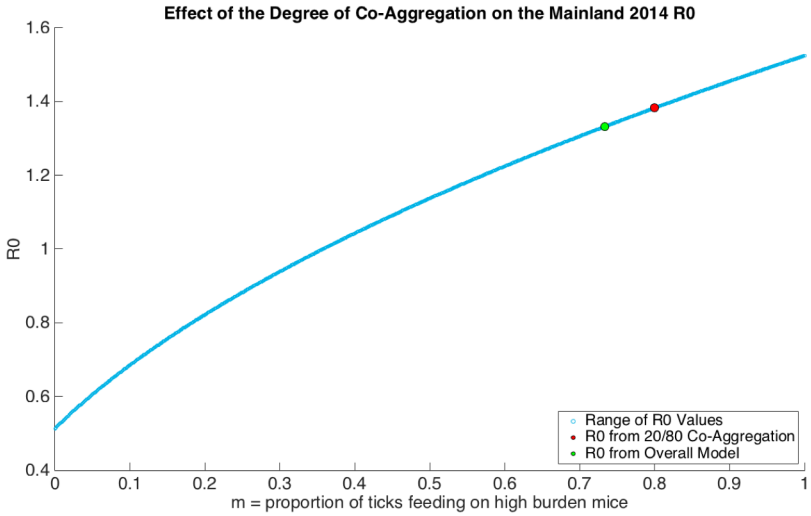

Figure 2. R_0 as a function of the degree of co-aggregation for the Island 2014 scenario

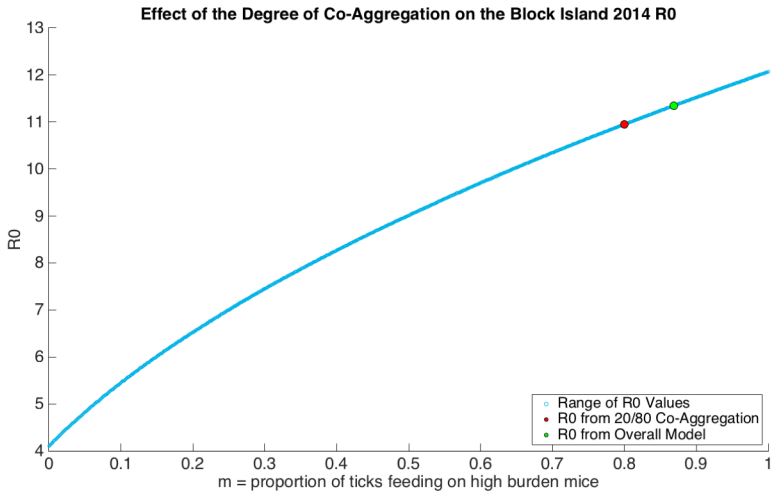

Figure 3. R_0 as a function of the degree of co-aggregation for the Island 2013 scenario

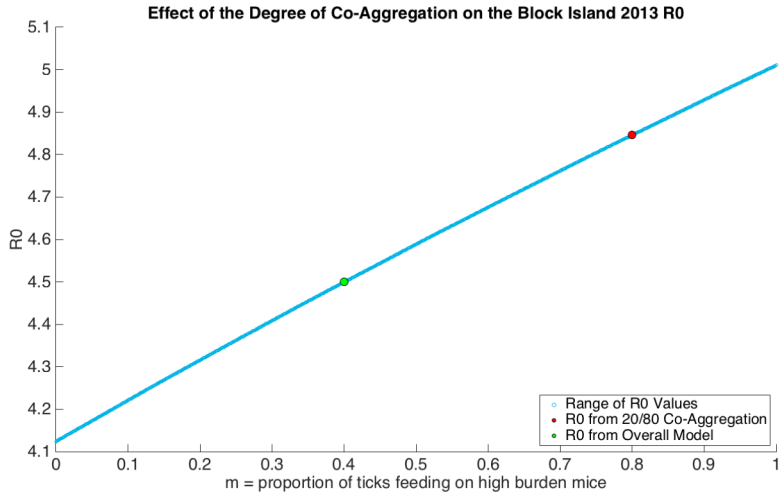

Figure 4. R_0 as a function of the degree of co-aggregation for the Island 2014 scenario with no spring larval activity

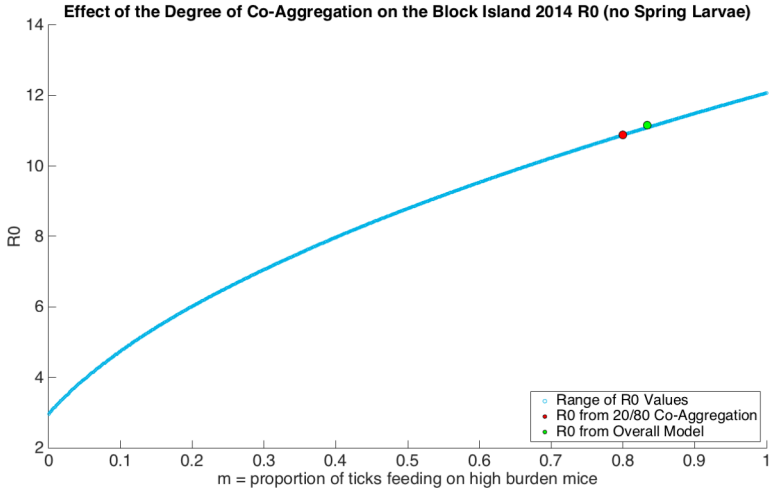

APPENDIX F.

Works Cited in Appendices A - E

Brunner, J. L., and R. S. Ostfeld. 2008. Multiple causes of variable tick burdens on small-mammal hosts. Ecology **89**:2259–2272.

Davis, S., and S. J. Bent. 2011. Loop analysis for pathogens: niche partitioning in the transmission graph for pathogens of the North American tick Ixodes scapularis. Journal of Theoretical Biology **269**:96–103.

Donahue, J. G., J. Piesman, and A. Spielman. 1987. Reservoir competence of white-footed mice for Lyme disease spirochetes. The American journal of tropical medicine and hygiene **36**:92–96.

Dunn, J. 2014. The mathematical epidemiology of human babesiosis in the north-eastern united states. Available from http://researchbank.rmit.edu.au/view/rmit:160817.

Dunn, J. M., S. Davis, A. Stacey, and M. A. Diuk-Wasser. 2013. A simple model for the establishment of tick-borne pathogens of Ixodes scapularis: a global sensitivity analysis of R0. Journal of Theoretical Biology **335**:213–221.

Gray, J. S. 1998. The ecology of ticks transmitting Lyme borreliosis. Experimental & Applied Acarology **22**:249–258. Kluwer Academic Publishers.

Hartemink, N. A., S. E. Randolph, S. A. Davis, and J. A. P. Heesterbeek. 2008. The basic reproduction number for complex disease systems: defining R(0) for tick-borne infections. The American naturalist **171**:743–754.

Kurtenbach, K., K. Hanincová, J. I. Tsao, G. Margos, D. Fish, and N. H. Ogden. 2006. Fundamental processes in the evolutionary ecology of Lyme borreliosis. Nature reviews. Microbiology **4**:660–669.

Main, A. J., A. B. Carey, M. G. Carey, and R. H. Goodwin. 1982. Immature Ixodes-Dammini (Acari, Ixodidae) on Small Animals in Connecticut, Usa. Journal of medical entomology **19**:655–664.

Main, A. J., H. E. Sprance, K. O. Kloter, and S. E. Brown. 1981. Ixodes-Dammini (Acari, Ixodidae) on White-Tailed Deer (Odocoileus-Virginianus) in Connecticut. Journal of medical entomology **18**:487–492.

Mather, T. N., M. L. Wilson, and S. I. Moore. 1989. Comparing the relative potential of rodents as reservoirs of the Lyme disease spirochete (Borreliaburgdorferi). American Journal of ….

Piesman, J., and A. Spielman. 1979. Host-associations and seasonal abundance of immature Ixodes dammini in southeastern Massachusetts. Annals of the Entomological ….

Piesman, J., and L. Gern. 2004. Lyme borreliosis in Europe and North America. Parasitology-Cambridge.

Rollend, L., D. Fish, and J. E. Childs. 2013. Transovarial transmission of Borrelia spirochetes by Ixodes scapularis: a summary of the literature and recent observations. Ticks and Tick-borne Diseases **4**:46–51.

Schoeler, G. B., and R. S. Lane. 1993. Efficiency of Transovarial Transmission of the Lyme-Disease Spirochete, Borrelia-Burgdorferi, in the Western Blacklegged Tick, Ixodes-Pacificus (Acari, Ixodidae). Journal of medical entomology **30**:80–86.

Spielman, A., M. L. Wilson, J. F. Levine, and J. Piesman. 1985. Ecology of Ixodes dammini-borne human babesiosis and Lyme disease. Annual review of entomology **30**:439–460.

Steere, A. C., J. Coburn, and L. Glickstein. 2004. The emergence of Lyme disease. The Journal of clinical investigation **113**:1093–1101.

Telford, S. R., III, T. N. Mather, S. I. Moore, M. L. Wilson, and A. Spielman. 1988. Incompetence of Deer as Reservoirs of the Lyme-Disease Spirochete. The American journal of tropical medicine and hygiene **39**:105–109.

Wilson, M. L. 1998. Distribution and abundance of Ixodes scapularis (Acari: Ixodidae) in North America: ecological processes and spatial analysis. Journal of medical entomology **35**:446–457.

Wilson, M. L., and A. Spielman. 1985. Seasonal activity of immature Ixodes dammini (Acari: Ixodidae). Journal of medical entomology **22**:408–414.
Wilson, M. L., J. F. Levine, and A. Spielman. 1984. Effect of Deer Reduction on Abundance of the Deer Tick (Ixodes-Dammini). The Yale journal of biology and medicine **57**:697–705.
Yuval, B., and A. Spielman. 1990. Duration and regulation of the developmental cycle of Ixodes dammini (Acari: Ixodidae). Journal of medical entomology **27**:196–201.